Master's thesis

A Study on Whole Blood Cryopreservation for Immunophenotyping by Flow Cytometry and Its Application on COVID-19 Research

Ngoc Anh Nguyen

International Master's program in Translational Medicine

Faculty of Medicine

University of Helsinki

October, 2021

UNIVERSITY OF HELSINKI

TABLE OF CONTENTS

Abbreviations

ACK	Ammonium-Chloride-Potassium
ACE2	Angiotensin-converting enzyme 2
ADCC	Antibody-dependent cellular cytotoxicity
APC	Antigen-presenting cell
ARDS	Acute respiratory distress syndrome
ARG1	Arginase 1
CD	Cluster differentiation
CLP	Common lymphoid progenitors
CM/ T_{CM}	Central memory T cells
CMP	Common myeloid progenitors
CMV	Cytomegalovirus
COVID-19	Coronavirus disease 2019
CST	Cytometer Set-Up and Tracking
CTL	Cytotoxic T lymphocytes
CXCL1	Chemokine (C-X-C motif) ligand 1
CyTOF	Cytometry by Time-Of-Flight
DAMPS	Damage-associated molecular patterns
DC	Dendritic cell
DMSO	Dimethyl sulfoxide
EDTA	Ethylenediaminetetraacetic acid
EFF	Effector cell
EM/T_{EM}	Effector memory T cells
EMRA/ T_{EMRA}	Terminally differentiated effector memory T cells
F/M	Female/Male
FACS	Fluorescence-activated cell sorting
FasL	Fas ligand
FC	Flow cytometry
FCS	Fetal calf serum
FlowSOM	Self-Organising Maps
fMLP	N-formylmethionine-leucyl-phenylalanine
FSC	Forward scatter
G-MDSC	Granulocytic myeloid derived suppressor cell
GMP	Macrophage progenitors
HIV	Human immunodeficiency virus
HLA	Human leukocyte antigen
HSC	Hematopoietic stem cells
HSV	Herpes Simplex Virus

ICU	Intensive care unit
ITAM	Tyrosine-based activation motif
ITIM	Immunoreceptor tyrosine-based inhibition motif
IVD	In-vitro diagnostic
LN	Lymph node
LPS	Lipopolysaccharides
M-MDSC	Monocytic myeloid derived suppressor cell
MDSC	Myeloid derived suppressor cell
MEP	Megakaryocyte and erythrocyte progenitors
MFI	Median fluorescence intensity
MHC	Major histocompatibility complex
Min	minutes
MMP	Matrix metalloproteinase
MPO	Myeloperoxidase
NET	Neutrophil extracellular traps
NK cell	Natural killer cell
PAMPS	Pathogen-associated molecular patterns
PB	Peripheral blood
PBMC	Peripheral blood mononuclear cell
PBS	Phosphate buffered saline solution
PD-L1	Programmed death-ligand 1
PMT	Photomultiplier tube
PPR	Pattern recognition receptors
PROT-1	Proteomic stabiliser
RBC	Red blood cells
ROS	Reactive oxygen species
rSD	Robust standard deviation
RT	Room temperature
RTE	Recent thymic emigrant
SARS-CoV-2	Severe acute respiratory syndrome-related coronavirus 2
SCM	Stem cell memory
SLSS-V2	Stable-Lyse V2 and Stable-Store V2
SSC	Side scatter
TCR	T cell receptors
UMAP	Uniform Manifold Approximation and Projection
wks	weeks
yrs	Years
γδ	Gamma-delta

Abstract

Immunophenotyping by flow cytometry (FC) is an established practice to identify immune cells and their cellular changes at the single-cell level. Since preserving the structural integrity of cellular epitopes is vital for immunophenotyping, samples should be processed shortly after being collected. However, the requirements of complex facilities and trained personnel for flow cytometry make it challenging to handle samples immediately. Fixation and cryopreservation extend sample shelf life and allow analysing longitudinal samples simultaneously while minimizing technical variation. Nevertheless, usage of whole blood cryopreservation in flow cytometry is limited due to challenges in preserving epitope structures during fixation and detecting dim antigens.

This thesis investigates the performances of four commercial whole blood cryopreserving kits; 1) Cytodelics, 2) Stable-Lyse V2 and Stable-Store V2 (SLSS-V2), 3) Proteomic stabiliser (PROT-1), and 4) Transfix. Peripheral blood samples were processed with these stabilising buffers immediately after the collection and cryopreserved until further analysis by flow cytometry. Here, we measured the stability of major immune lineages, T cell subpopulations, and activated neutrophil profiles in samples treated with these commercial whole blood stabilisers.

Our flow cytometry data showed that PROT-1, Transfix and Cytodelics maintained the distribution of major leukocyte subsets – granulocytes, T cells, natural killer cells and B cells, comparable to unpreserved samples despite the attenuation of fluorescence intensities. Moreover, these three stabilisers also preserved phenotypes of activated neutrophils upon stimulation with N-Formylmethionyl-leucyl-phenylalanine and Lipopolysaccharides. The upregulation of adhesion molecules (CD11b), Fc receptors (CD16) and granule proteins (CD66b) as well as the shedding of surface L-selectin (CD62L) on activated neutrophils was conserved most efficiently in PROT-1, followed by Cytodelics. On the other hand, none of the stabilisers provided a reliable detection of CCR7 for accurate quantification of T cell subpopulations.

COVID-19 is caused by a highly transmissible and pathogenic coronavirus, so-called severe acute respiratory syndrome coronavirus 2 (SARS-COV-2). To test the potential of whole

blood cryopreservation kits for flow cytometry in COVID-19 research, we studied the detectability of major leukocyte lineages and granulocyte subsets in longitudinal patient samples processed with Cytodelics. High dimensional analysis with Uniform Manifold Approximation and Projection (UMAP) and Self-Organising Maps (FlowSOM) clustering revealed remarkable stability of CD3, CD15, and CD14 expression in samples stored with Cytodelics. It allowed the detection of lymphopenia and emergency granulopoiesis often found during the acute phase of severe SARS-COV-2 infection. Nonetheless, we could not determine signatures of granulocyte subsets, notably suppressive neutrophils, during the acute and convalescent phases of COVID-19. Variable detection of lowly expressed markers and diminished fluorescence intensities in Cytodelics - preserved samples might have hindered the analysis.

In conclusion, this study demonstrates that PROT-1, Transfix, and Cytodelics enabled reliable detection of highly expressed leukocyte markers, whereas SLSS-V2 preservation resulted in the most inaccurate identification of studied markers. Notably, our results show that Cytodelics can be applied in COVID-19 studies to immunophenotype major immune lineages by flow cytometry. Nevertheless, more optimisation is needed for less abundant or fixation-sensitive epitopes to enhance the efficacy of whole blood cryopreservation for flow cytometry.

1. Introduction

1.1. Immunophenotyping

1.1.1. Definition and methods

Identifying immune cells and screening for their changes – so-called immunophenotyping, are fundamental in clinical and research work. With immunophenotyping, it is possible to measure the expression of both intracellular and surface antigens by labelling them with antibodies conjugated with signal molecules, ranging from fluorescent proteins in flow cytometry to rare metals in mass cytometry. Gene expression analysis is a more state-of-the-art method, providing a broader view of the immune landscape. However, high-cost and complex gene expression analysis and mass cytometry facilities make flow cytometry still more accessible and preferable in clinics and many laboratories. In addition, immunophenotyping by flow cytometry allows isolating specific cell populations for deeper transcriptomic studies[1]. Moreover, most biological samples such as blood, bone marrow, or tissues can be used for immunophenotyping, making the technique versatile for a wide range of clinical assessments and studies.[2–4]

1.1.2. Application

In clinical use, immunophenotyping allows physicians to detect and make an initial assessment of immune responses against diseases and evaluate the efficacy of the treatments. Routine immunophenotyping tests are commonly used in diagnosis and monitoring treatment and prognosis of cancers of hematopoietic origin, such as leukaemia, lymphoma, and myeloma. By simultaneously measuring multiple markers at the single-cell level, immunophenotyping by flow cytometry can enumerate and determine cell lineage, clonality, proliferation, or activation status of neoplastic cells. This information helps identify subgroups of blood cancer, evaluate patients' responses to different treatments and monitor for the occurrence of minimal residual disease[5]. Information about enumeration and functional markers of several immune subsets also aids in diagnosing immunodeficiency diseases and uncharacteristic inflammatory symptoms[6].

Immunophenotyping is also the standard procedure in most of hepatology, immunology, and oncology research laboratories. It helps researchers characterise the

immune landscape of the studied materials and detailed information about expression patterns of several cellular proteins simultaneously. Moreover, immunophenotyping is a crucial part of clinical studies on immunotherapies to understand how much new treatments can boost or hinder immune responses and what the underlying mechanism might be.[7,8]

1.2. Immune system

1.2.1. Innate and adaptive immunity

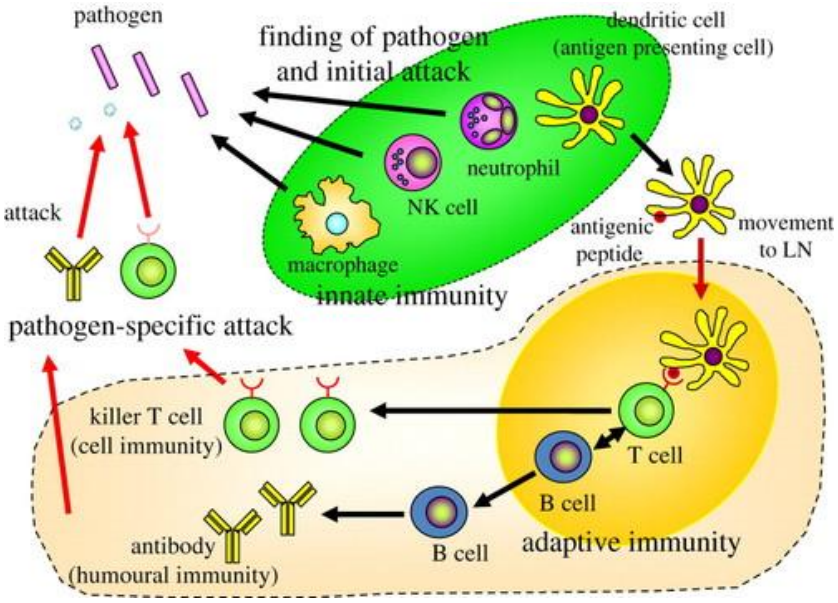

Figure 1: Overview of innate and adaptive immunity. Innate cells (green) recognise and phagocyte pathogens rapidly using pre-programmed receptors. Antigen-presenting cells such as dendritic cells then process and present pathogen antigens to T lymphocytes in lymph node (LN) and trigger adaptive immunity (yellow). As a result, activated T and B cells mount pathogen-specific attacks. Reproduced with permission from reference.[9]

Two major systems, innate and adaptive immunity, work closely together to fight off infection. Upon encountering microbes, pattern recognition receptors (PPRs) expressed by innate immune cells such as neutrophils or macrophages can recognise pathogen-associated molecular patterns (PAMPs) such as bacterial lipopolysaccharides (LPSs) and endotoxins. Upon binding to bacterial molecules, resident macrophages and neutrophils will phagocyte the bacterium and secrete proinflammatory cytokines and chemokines, triggering inflammation and attracting other immune cells. Local inflammation and phagocytosis of bacteria also activate complement system, a tightly regulated network of proteins. Upon

activation, complement system can opsonize, recruit phagocytes and trigger bacteria lysis.[10,11] (Figure 1)

After about seven days of infection, adaptive immunity is subsequently activated by antigen-presenting cells, such as dendritic cells (DC). After ingesting microbes, tissue-resident DCs migrate to lymph nodes and present pathogen antigens to T lymphocytes. These DCs also provide co-stimulatory signals and cytokines needed to activate T cells. T cell activation results in clonal expansion and differentiation, generating effector cells and immunological memory specifically targeting pathogens of interest. Generated T cell subsets play a diverse function, e.g. activating B cells, destroying infected cells, enhancing phagocyte functions, worsening or resolving inflammation.[12,13] (Figure 1)

1.2.2. Major immune cells

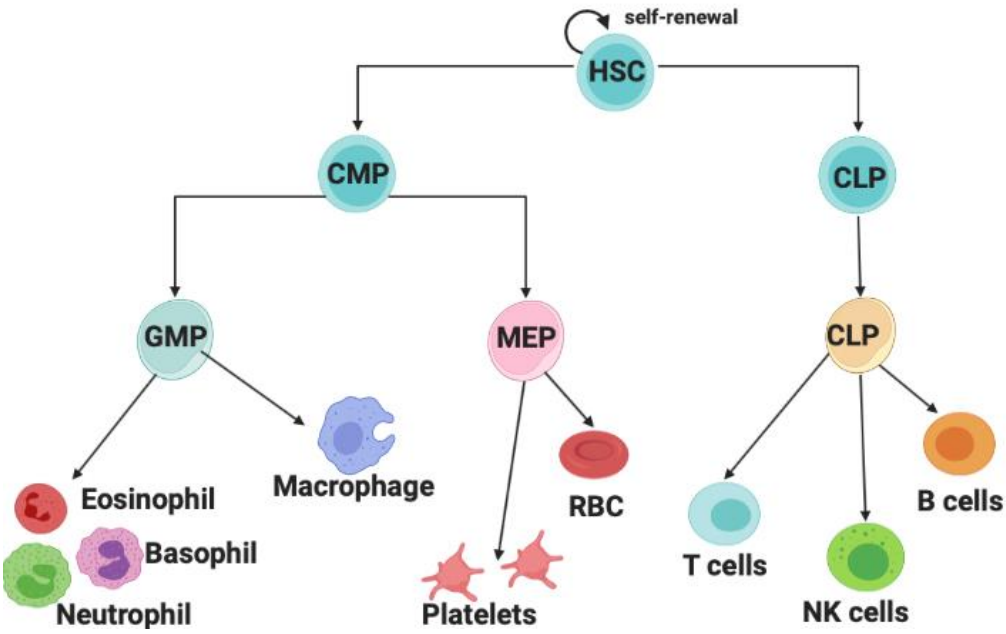

Figure 2: Major immune subsets. Hematopoietic stem cells (HSC) have the capacity of self-reviewing and differentiating into common myeloid progenitors (CMP) and common lymphoid progenitors (CLP). CMPs then differentiate into granulocyte and macrophage progenitors (GMP) and megakaryocyte and erythrocyte progenitors (MEP). These progenitors give rise to mature peripheral blood cells, as indicated at the bottom. RBC - red blood cell; NK - natural killer cells. The image was generated with Biorender.com and produced based on reference.[14]

Immune cells are the most active players of the immune system - our natural defence against pathogens or harmful physiological changes. They are originated from hematopoietic stem cells in the bone marrow. Depending on signal and timing, they can differentiate into common myeloid progenitors (CMP) and common lymphoid progenitors (CLP). The first subgroup develops into thrombocytes, red blood cells (RBC), and most innate immune cells such as eosinophil, neutrophil, basophils, and monocytes, each of which can possess a wide range of innate receptors to recognise and eliminate pathogens upon encountering. Except for natural killer cells and dendritic cells, most common lymphoid progenitors become either B cells (bone marrow-derived cells) and T cells (thymus cells), which require activation from innate immune system for effector functions and clonal expansion against pathogens as well as generating immunological memory (Figure 2).

1.2.2.1. Monocytes

Monocytes are the largest human leukocytes, making up only 2 to 10% of total circulating immune cells under normal conditions, but they are critical professional phagocytes and antigen-presenting cells. Monocytes are classified into three subgroups, namely classical, intermediate, and non-classical, depending on the expression of CD14 and CD16. The largest subgroup, classical monocytes defined as $CD14^{++}CD16^{-}$, are scavenger cells, removing bacterial pathogen and dying cells via phagocytosis. They can also activate or control other immune cells by producing proinflammatory cytokines. In addition, they can infiltrate tissues and differentiate into dendritic cells or sometimes macrophage[15,16]. On the other hand, intermediate and non-classical monocytes, defined as CD14+CD16+ and $CD14^{-}CD16^{+}$ respectively, are more pro-inflammatory. Their primary functions are patrolling for injury, secreting a large number of proinflammatory cytokines, presenting antigens to T cells, and differentiating into antigen-presenting cells such as dendritic and macrophages.[17]

In a clinical setting, measuring an absolute number of monocytes is part of routine blood tests. An elevated number of monocytes can indicate bacterial, viral, or parasitic infections, but also non-infectious diseases characterized by chronic inflammation such as inflammatory bowel syndrome, rheumatoid arthritis, or certain leukemia[16,18]. On the other hand, sepsis, aplastic anaemia or chemotherapy can cause monocytopenia, a condition with an abnormally low number of monocytes[19,20].

1.2.2.2. Granulocytes

The most abundant immune cells in circulation are granulocytes, which include neutrophils, basophils, and eosinophils. Cytoplasmic granules and segmented nuclei are the main features to characterise them. Upon infection, neutrophils and eosinophils can release cytotoxic granules, phagocyte pathogens and mediate inflammation. In comparison, basophils are more active in allergy.

This study focuses on neutrophils since they account for up to 70% of circulating immune cells. There are about one billion neutrophils produced per kilogram of body weight each day, and this number can increase up to 10 billion cells during infection[21]. Developed in bone marrow, neutrophils are released into the circulation upon maturation. Without infection, their half-life is just about 6 to 8 hours[22]. Early signs of infection or inflammatory diseases can also be detected through the number of circulating neutrophils, which is routinely measured in a complete blood count.

1.2.2.3. Neutrophil recruitment and activation

Neutrophils are recruited to infected sites by proinflammatory factors and chemotactic stimuli triggered by pathogen-associated molecular patterns (PAMPs) and damage-associated molecular patterns (DAMPs). These factors are, e.g. IL-8, IL-17, bacteria-derived N-formylmethionine-leucyl-phenylalanine (fMLP), complement protein C5a, CXCL1, and CXCL2. Once released, they induce changes in surface proteins of the endothelium and subsequently lead to tethering and transmigration of the free-flowing neutrophils to the infected site.[23]

In addition to host-derived stimuli and chemoattractants at the inflamed site, neutrophils can also be directly activated by PAMPs and DAMPs such as fLMP and LPS, which can bind directly to a repertoire of PPRs on neutrophils such as toll-like receptors, C-lectin like receptors, and NOD-like receptors. The binding triggers the MAPK/ERK signalling cascade, resulting in neutrophil effector functions such as oxidative burst and degranulation[24]. Neutrophil activation alters expression of cell surface receptors, such as upregulation of

integrin family (CD11b), Carcinoembryonic antigen-related cell adhesion molecule 8 (CD66b), complement receptor 1 (CD35), or downregulation of L-selectin (CD62L).[25] (Figure 3)

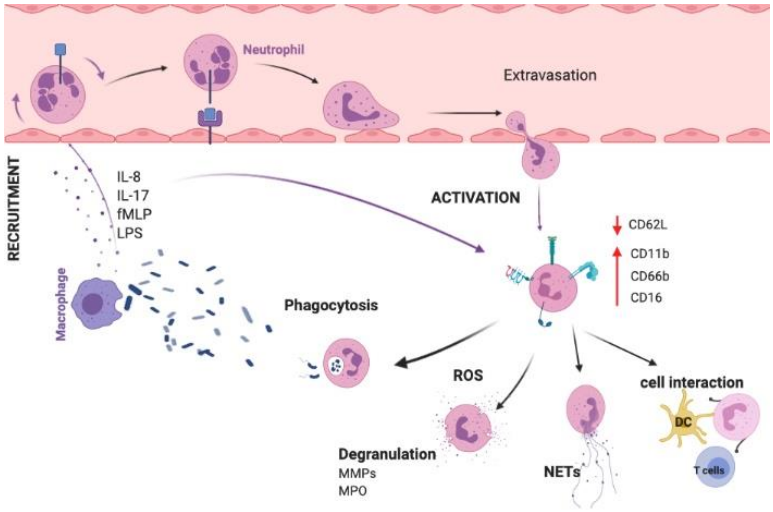

Figure 3: Overview of neutrophils recruitment, activation, and functions. Pathogen-associated molecular patterns (PAMPs), damage-associated molecular patterns (DAMPs), and inflammatory cytokines make endothelial cells more permeable and trigger neutrophil recruitment and activation. Activated neutrophils then induce pathogen clearance by phagocytosis or production of reactive oxygen species (ROS) and neutrophil extracellular traps (NET), which can trap and limit the spread of the infection. In addition to that, released granules contain a diverse range of molecules such as myeloperoxidase (MPO) and matrix metalloproteinase (MMPs) to modulate inflammation. Neutrophils also play a necessary function in mediating adaptive immunity by interacting with T lymphocytes. fMLP, bacteria-derived N-formylmethionine-leucyl-phenylalanine; LPS, bacterial lipopolysaccharides.

1.2.2.4. **Neutrophil effector functions**

Upon activation, neutrophils play a diverse role in pathogen clearance, inflammation resolution, tissue damage, and autoimmunity. They are a complex and heterogeneous cell population, consisting of both pro-inflammatory and immunosuppressive subsets. During the infection, degranulated neutrophils release proteolytic enzymes, antimicrobial peptides, or inflammatory molecules such as collagenases for neutrophil extravasation, myeloperoxidase for ROS production, or alpha-defensins directly targeting bacteria. Granule peptides such as cathelicidins can also participate in both antimicrobial and immunomodulatory activities.[23,26]

In addition to degranulation, neutrophils can phagocyte pathogens opsonised by antibodies and induce oxidative burst, which causes damage directly to the pathogen,

enhance antiviral response and promote neutrophil extracellular traps (NET). These are web-like chromatin structures embedded with neutrophilic granule proteins, capable of neutralising and destroying bacteria, fungi, or viruses.[27,28]

Neutrophils are not solely efficient at eliminating microbial pathogens, but they also modulate other immune cell responses. For example, degranulating neutrophils can present antigens or release factors promoting T cell proliferation, whereas resting neutrophils can have immune-suppressive function depending on types of infection[29]. Neutrophils can also act as antigen-presenting cells to memory $CD4^+$ T cells and induce the production of antimicrobial antibodies.[30,31,] (Figure 3)

1.2.2.5. Suppressive neutrophils

Traditionally, suppressive neutrophils refer to myeloid-derived suppressor cells (MDSC). They are immature myeloid cells, which produce a high level of reactive oxygen species and arginase I to suppress T lymphocytes during pathological conditions such as cancer or infection[32–34]. Traditionally, human MDSCs are isolated from peripheral blood mononuclear cell (PBMC) fraction and subdivided into *granulocyte-like MDSC* (G-MDSC) described as $Lin^-HLA\text{-}DR^{low}CD11b^+CD15^+CD14^-$ and *monocytic MDSCs* (M-MDSC) as $Lin^-HLA\text{-}DR^{low/-}CD11b^+CD33^+CD14^{+33}$. However, despite attempts to define G-MDSC over the years, there is no good marker or consensus on how to distinguish them from other suppressive neutrophils yet.

Since Gabrilovich et al. proposed the term MDSC in 2007[32], different granulocyte subsets were found to have overlapping suppressive features of MDSC, such as mature low-density neutrophils[35,36]. Some studies suggested that G-MDSC is 'a phenotype of neutrophils'[37] or a subpopulation of degranulating granulocytes[38]. In other words, MDSCs or more specifically G-MDSCs can be considered as a heterogenous subgroup of suppressive neutrophils. They are increased especially during emergency myelopoiesis - a situation where immature and mature myeloid cells are generated rapidly in response to inflammation[39]. Thus, G-MDSC properties can manifest depending on the physiological cues regardless of their maturity.

1.2.2.6. **Mechanism of immune suppression**

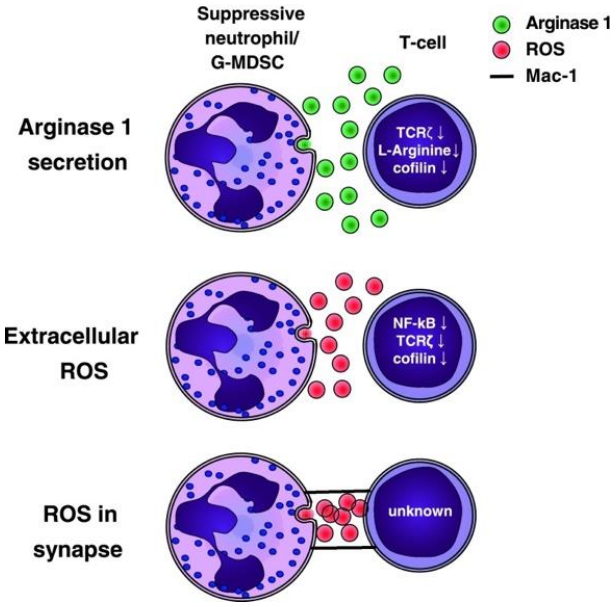

Figure 4: Mechanism of suppression by MDSCs and suppressive neutrophils. Arginase 1 (ARG1) and reactive oxygen species (ROS) can induce suppression by multiple pathways. G-MDSC, granulocytic myeloid derived suppressor cell. Reproduced with permission from reference.[37]

G-MDSC and neutrophils can suppress T cell responses by releasing arginase-1 (ARG1) to interrupt T cell proliferation and activation. Arginase-1 released from the gelatinase-containing granules depletes L-arginine in the microenvironment by converting them to l-ornithine and urea[37,40]. In an L-arginine-derived microenvironment, T cell proliferation is arrested at G0-G1 phase[41]. ARG1 also mediates the attenuation of T cell activation by disrupting the recycling of TCR/CD3 complex and the reorganisation of actin cytoskeleton for immunological synapse formation[42]. Taken together, ARG1 can profoundly inhibit T cell function, and interestingly, overcoming arginine depletion has been shown to reconstitute T cell proliferation and boost immunotherapy in tumor microenvironment[43,44](Figure 4).

Production of reactive oxygen species (ROS) is another mechanism utilised by suppressive neutrophils or G-MDSCs. Like ARG1, oxidative stress interferes with the actin depolymerisation and recycling of TCR/CD3, thus blocking T cell function. A high level of ROS also induces T cell hypo-responsiveness by inhibiting NF-κB as well as triggering T cell apoptosis through Fas/FasL pathway[45].

1.2.3. Lymphocytes

1.2.3.1. Natural Killer cells

A small portion of lymphoid progenitors differentiates into natural killer (NK) cells, an innate lymphocyte population. NK cell activation depends on activating and inhibitory receptors associated with immunoreceptor tyrosine-based activation motif (ITAM) and immunoreceptor tyrosine-based inhibition motif (ITIM), respectively. The activation occurs when the balance between inhibitory and activating signals is broken. In humans, they are subdivided into two main populations based on CD16 and CD56 expression - $CD56^{dim}$ and $CD56^{bright}$. $CD56^{dim}CD16^{bright}$ are considered cytotoxic ones since they mediate both natural and antibody-dependent cellular cytotoxicity (ADCC). The $CD56^{bright}$ $CD16^{dim/-}$ subgroup is regarded as a cytokine producer and the precursor of the $CD56^{dim}$ cytotoxic subset. NK cell deficiency can cause severe Cytomegalovirus (CMV) and Herpes Simplex Virus (HSV) infection.[46–49]

1.2.3.2. B cells

B cells, defined as $CD19^{+}$, are the only cells that can produce antibodies and mediate humoral immunity. Naïve B cells harbour immunoglobulin receptors, mostly M and D type, which can bind diverse kinds of antigens, such as microbial proteins, lipids, polysaccharides, nucleic acids, and chemical toxins. B lymphocytes are activated upon antigen recognition and external signals, such as from T helper cells or complement system. Once activated, these cells undergo clonal expansion, giving rise to antibody-secreting plasma cells, high-affinity Ig expressing cells, or memory cells. After the first exposure with a protein antigen, long-lived plasma cells and memory cells return to the bone marrow and stay dormant there for a long time. These cells ensure more rapid and efficient responses in the subsequent exposure by producing a more significant number of antibodies and faster affinity maturation of the antibodies produced. Activated B cells can also undergo isotype switching, generating different types of antibodies with the same specificity, resulting in more effective immune responses against certain pathogens.[50,51]

1.2.3.3. **T cells**

Originated from bone marrow, thymus-seeding progenitor cells migrate to thymus to mature and differentiate into thymocytes that will eventually become mature T cells. Central event in the maturation of thymocytes is the gene rearrangement to generate T cell receptors (TCR). After the TCR rearrangement, T cells must pass negative and positive selection, meaning that they can tolerate self-structures and have sufficient affinity for self-major histocompatibility complex (MHC) or human leukocyte antigen (HLA) in humans. Two dominant lineages that emerge from thymus are categorized based on their co-receptors expressed as CD4 – T helper cells, and CD8 – cytotoxic cells.[12]

1.2.3.3.1. CD4 and CD8 T cells

CD4 T helper cells are actively involved in the regulation of both innate and adaptive responses. Depending on the type of activation and cytokine signalling they receive, CD4 T cells can differentiate into distinct subsets. Each subset subsequently activates or modulates activities of specific immune cells, depending on types of pathogens. Also, CD4 cells exhibit both pro-inflammatory and immunosuppressive functions.[52,53]

CD8 cells – cytotoxic T lymphocytes (CTL) are the prominent "foot soldiers of the immune system"[54]. Upon engaging with MHC-Class I bearing known pathogenic antigens, CD8 cells rapidly destroy infected cells by releasing cytotoxic granules containing perforins and granzymes. Subsequently, the caspase cascade will be activated in the infected cells, resulting in cell death. CTLs can also induce cell death through the Fas-FasL pathway, particularly to maintain immune homeostasis.[12,55,56]

Classical T cells egress from the thymus as naïve cells and enter circulation. Among naïve cells, recent thymic emigrants (RTEs) are the youngest T cells, which are the most recent cells entering the lymphoid periphery. RTEs are an indicator of thymic output and a critical parameter maintaining the peripheral pool of diverse T cells. Their capacity of proliferation and cytokine production is lower compared to mature naïve cells. In human, platelet endothelial cell adhesion molecule known as CD31 is used to identify RTEs. Understanding RTEs and thymic output is essential in monitoring immunodeficiencies or immune-reconstitution after hematopoietic stem cell transplantation.[57–59]

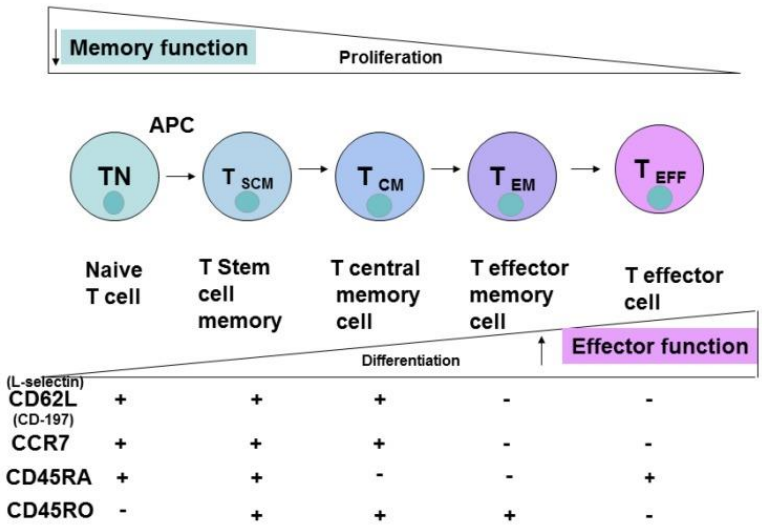

Figure 5: Different subsets of circulating T cells. Each subgroup has a different capacity of differentiation and proliferation. CD62L and CCR7 are the primary receptors for trafficking to secondary lymphoid tissues. SCM, stem cell memory; CM, central memory; EM, effector memory; EFF, effector; APC, antigen-presenting cell. Reproduced with permission from reference[52].

Mature naïve T cells migrate to secondary lymphoid tissues. There, they can be activated only after receiving all three distinct signals: (1) recognition of antigen-HLA complex, (2) specific antigen co-stimulation and (3) appropriate cytokines for activation and proliferation[60]. Upon activation, T cells will proliferate and differentiate into effector and memory cells bearing the same antigen specificity. After re-entering the circulation, the effector cells migrate to the infected area to clear out infection while the memory cells survey lymphatic tissues for the same pathogenic antigen.[12]

There are three main subsets of memory cells, depending on expression of CD45RO, CD45RA, and CCR7 (Figure 5). Effector memory (T_{EM}) can enter the infected site by expressing different integrins and chemokine receptors such as CCR5. They are active in the immediate adaptive response by producing a large number of effector cytokines and perforin[61]. On the other hand, the central memory cells (T_{CM}) express peripheral homing receptors such as CCR7 and CD62, making them more restricted to secondary lymphoid tissues. While providing primary immunosurveillance of known pathogens, T_{CM} cells can rapidly proliferate and give rise to both effector and T_{EM} cells. Another subset of memory, so-called terminally differentiated effector memory cells (T_{EMRA}), re-expresses CD45RA. It is not clear about the

functions of T_{EMRA} cells, which express markers for senescence and have low functional and proliferative capacity. Figure 5 gives a summary of these subsets and their corresponding surface markers.[52,61]

1.2.3.3.2. Gamma delta T cells

Gamma-delta (γδ) T cells, characterised by their unique expression of γδ TCR, are non-conventional cells, accounting for less than 5% of total circulating lymphocytes. Nonetheless, they are more abundant in peripheral tissues such as the skin and gut mucosa. In addition, γδ T cells resemble conventional alpha-beta (αβ) T cells regarding their cytotoxic activities and cytokine production. However, unlike αβ cells, γδ T lymphocytes' functional responses are independent of MHC molecules and antigen-presenting cells.[62]

γδ T cells can recognize a wide range of pathogenic and stress antigens and display NK-like effector functions. Moreover, they are capable of processing antigens and cross-presenting them to conventional T cells and other immune cells. In addition to immune surveillance of infection and tumor microenvironment, γδ T cells also contribute to the homeostasis of tissue physiology and control neuronal synaptic plasticity in the central nervous system. Aberrant activities of γδ T were found in autoimmune diseases (e.g. systemic sclerosis) and infection such as human immunodeficiency virus (HIV) infection. Thus, phenotyping γδ T cells is essential given their diverse subsets and functions.[62–64]

1.3. Immune responses during SARS-COV-2 infection

As of September 2021, SARS-CoV-2, a pathogenic coronavirus, has claimed more than 4.5 million lives globally since it emerged in 2019 in Wuhan, China. Being a single-stranded RNA virus, SARS-CoV-2 can cause a wide range of clinical manifestations, depending on an individual's age and co-morbidities. While young and healthy people most often experience mild to moderate disease, some with pre-existing medical conditions and impaired immune system can develop severe respiratory illness, many of whom have succumbed to death.[65–67]

1.3.1. Immunopathogenesis

To enter host cells, the spike protein of SARS-CoV-2 binds to angiotensin-converting enzyme 2 (ACE2) that is abundantly expressed on airway epithelial cells[68]. Host TMPRSS2 enzyme then cleaves the spike protein, allowing the viral membrane to fuse with the host cells[69]. At the end of its replicating cycle, SARS-CoV-2 induces death and injury in the infected host cells, a majority of which are lung epithelial cells. SARS-CoV-2 is linked to pyroptosis, a highly inflammatory form of cell death, which results in proinflammatory cytokine secretion[70]. In healthy individuals, this is a signal for the recruitment of immune cells, such as T lymphocytes, to clear out the infection and resolve the inflammation. However, an impaired immune system might lead to a massive level of cytokines released and unrestrained immune cell infiltration to the lungs, which might be a reason for the lymphopenia often seen in COVID-19 patients. These infiltrated cells produce an excessive amount of reactive oxygen species and proteases that mediate the lung damage further[66]. In addition, SARS-CoV-2 viral proteins can antagonise the host interferon responses, helping the virus escape innate immunity[71]. Taken together, it is crucial to understand the host responses since the severity of SARS-CoV-2 is not only from the viral infection itself but also from the dysfunctional immune reaction.

1.3.2. Neutrophils and challenges of studying them in the context of COVID-19

Accounting for up to 70% of the total circulating immune cells, neutrophils play an active role in both resolving and worsening the SARS-CoV-2 infection. Increased neutrophil to lymphocyte ratio is an indicator of a poor outcome in COVID-19[72]. There is an increase in both circulating and lung-infiltrated neutrophils. Their activation and degranulation markers are also increased[73]. Notably, severe cases displayed an expansion of immature and low-density neutrophils. Many of these cells are suppressive and can dampen the adaptive immune cell responses[72]. Together with activated neutrophils, these cells also release a high level of NETs, triggering immunothrombosis and possibly mediating acute respiratory distress syndrome (ARDS)[74]. There are still many remaining questions about the driving forces of aberrant neutrophil responses, NETs formation, and clearance during the SARS-CoV-2 infection.

To answer those questions, collecting high-quality samples is the first step. Since neutrophils are short-lived, easily activated upon blood drawing, and very sensitive to cryo-preservation, it is crucial to have a reliable method to stabilise samples immediately after being taken. Fresh blood samples or PBMC fractions are often used in neutrophil studies so far. Though they allow investigating neutrophil heterogeneity in depth, PBMC isolation process can alter neutrophil characteristics. On the other hand, processing fresh samples individually is demanding due to logistic and technical requirements, particularly during the pandemic.[73,75,76]

In addition, COVID-19 sample processing is challenging because SARS-CoV-2 is highly transmissible through droplets, aerosols, and fomites[77]. In other words, there is a need for a method that ensures both sample quality and staff safety. Here, we aimed to study whether commercially available whole blood stabilisers are suitable to study neutrophils with flow cytometry, which is the most popular immunophenotyping method globally.

1.4. Cryopreservation

Cryopreservation uses sub-zero temperatures to preserve the integrity and even viability of organelles, cells, tissues, or organs over a long period. Depending on types of samples and nature of research projects, cryogenic temperatures can range from –4°C to –140°C. At these temperatures, most of the biological activities are either reduced or stopped, preventing further changes or destruction of cellular structures. These features are critical to maintain intact cellular characteristics after removing cells from their physiological environment. Because of this, the method is widely used in clinics and research. Moreover, cryopreservation allows a considerable number of patient samples to be collected prospectively and analysed simultaneously to reduce technical variation and batch effects.[78]

Despite being widely used and optimised, cryopreservation of human samples efficiently is still challenging. During the freezing process, ice crystal formation and osmotic shock can damage cellular membranes, thus reducing samples' viability and quality. To minimise these cryo-damages, cryoprotectants such as Dimethyl sulfoxide (DMSO) and glycerol are often added to the freezing media. In addition to that, freezing containers with a

cooling rate of –1°C per minute can be used to reduce cellular damage due to temperature shock.[78]

Compared to other immune cells, granulocytes are particularly sensitive to the freezing process, and thus they are recommended to be analyzed within 2-4 hours of collection[79]. Clinical samples are often collected in hospitals and transferred to a separate flow cytometry unit for processing. Due to the logistics, analysing clinical samples within the recommended time frame of 4 hours is not always possible. Moreover, variation in sampling dates, handling personnel, and delaying time between sample collection and analysis can generate batch effects.

Moreover, sample processing can disrupt both chemical and mechanical homeostasis of granulocytes. Upon sensing those stimuli, neutrophils can switch between their activation or deactivation status[80]. Therefore, minimal intervention and gentle treatment are needed to preserve neutrophil properties. Cryoprotectants such as glycerol, osmotic stress, and cold shock during cryopreservation can significantly damage the neutrophils, resulting in the loss of functions and low viability[81,82]. Though limited to immunophenotyping only, fixation prior to cryopreservation of whole blood might retain neutrophil properties better than multi-step procedures.

2. Aims and hypothesis

This thesis project aims to compare the performance of different whole blood cryopreservation for immunophenotyping by flow cytometry using stabilising reagents commercialised primarily for mass cytometry – Cytodelics (Cytodelics AB, Stockholm, Sweden), Stable-Lyse V2 and Stable-Store V2 (SLSS-V2), and Proteomic stabiliser (PROT-1) (Smart Tube Inc., San Carlos, CA, US). As flow cytometry and mass cytometry both measure physical and chemical properties of single cells using antibodies, we hypothesised that these cryopreserving reagents should maintain cellular characteristics comparable to fresh samples and sufficient for measurements in flow cytometry.

Our objectives are as follows:

1. Determine the suitability of Cytodelics, SLSS, and PROT-1 for preserving general surface markers of different cell lineages – lymphocytes, monocytes, and granulocytes,

2. Study variables that might affect the sample quality before and after freezing, such as variations in sample processing, antibody clones and experimental workflow.

3. Evaluate the effects of stabilising reagents on neutrophils and their activation markers,

4. Assessing the feasibility of using Cytodelics for a longitudinal analysis of COVID-19 immune responses.

5. Explore how different subsets of neutrophils, specifically suppressive subtype including myeloid-derived suppressor cells (MDSC), change throughout the disease and how these changes might be associated with the outcome of COVID-19.

3. Materials and Methods

3.1. Clinical samples and patient characteristics

3.1.1. For whole blood cryopreservation study

Peripheral blood (PB) samples were collected by venepuncture to BD Vacutainer® EDTA tubes. Within 3 hours after the venesections, samples were added to cryo-tubes containing whole blood stabilising reagents and further processed according to manufacturers' recommendations.

3.1.2. For longitudinal study in COVID-19

Table 1: COVID-19 patient characteristics

Characteristic	Hospitalised	ICU
Characteristics		
Total number	8	7
Age (yrs)	59 [34 - 65]	58 [46 - 69]
Gender (F/M)	6 (86%) / 1 (14%)	3 (43%) / 4 (57%)
Hospitalisation days	6 [4 - 15]	15 [10-38]
Comorbidities		
Asthma (n)	4 (57%)	1 (14%)
Hypertension (n)	1 (14%)	1 (14%)
Obesity (n)	1 (14%)	4 (57%)
Cardiovascular disease (n)	NA	2 (29%)
Obstructive sleep apnea (n)	1 (14%)	2 (29%)
Diabetes (n)	NA	2 (29%)

Data are reported as median with range or number (%). ICU, intensive care unit. F/M, Female/male.

Patients hospitalized due to COVID-19 at the Helsinki University Hospital, Helsinki, Finland were invited to participate in the study. Inclusion criteria were SARS-CoV-2 infection confirmed by polymerase chain reaction test. However, patients undergoing immunosuppression treatment (e.g. Dexamethasone) were excluded from the study. PB samples were collected by venepuncture to BD Vacutainer® EDTA/ heparin blood collection tubes. 0.5ml PB samples were incubated with 0.5ml Cytodelics's stabiliser at RT for 10 minutes and then stored at -80°C.

All clinical samples were subgrouped based on severity. Hospitalised samples indicated milder cases, whereas subjects admitted to intensive care unit (ICU) were considered severe cases. Sampling taken within 15 days from symptom onset was categorised as the acute, whereas samples taken after 90 days were assigned to the convalescent group. However, three samples of the hospitalised cohort which were taken less than 90 days (specifically after 22, 61 and 77 days from symptom onsets) were included in the analysis as convalescent samples. Table 1 summarizes the characteristics of patient samples.

3.2. Ethical statement

The study was approved by the Ethics Committee of the Hospital District of Helsinki and Uusimaa (HUS/853/2020 and HUS/747/2019). All samples were taken with informed consent.

3.3. FACS Lysis solution

Fresh blood samples were stained with fluorochrome-conjugated antibodies for 25 minutes at RT and subsequently subjected to 1X BD Facs Lysing in 10 minutes at RT. Cells were washed twice with FACS staining buffer (2% FCS + 2mM EDTA in PBS) before being acquired on the flow cytometer

3.4. Whole blood cryo-preservation and thawing

Table 2: Overview of four commercial whole blood cryopreservation kits with BD Facs Lysing solution used as a fresh control

	BD Facs Lysing (Fresh & unpreserved)	**Cytodelics**	**PROT-1**	**SLSS-V2**	**Transfix**
Erythrocyte lysis	yes	yes	yes	yes	yes
Formaldehyde fixation	10%	< 5 %	3-7%	unknown	<1%
Methanol permeabilisation	3.50%	unknown	unknown	unknown	unknown
Cryoprotectant	unknown	unknown	3-7% Diethylene glycol	unknown	unknown
Freezing time (min)	-	10	10	30	15
Preserving temperature	-	-20 or -80	-80	RT/+4/-80°C	+4°C
Storage duration	-	1 yrs	13 months[83]	>2wks at +4°C unknown at -80°C	14 days
Thawing/RBC lysing (min)	-	30	～50	～10	～15

3.4.1. **Cytodelics (Cytodelics AB, Sweden)**

Stabilisers were calibrated at RT for 5 minutes before mixing with the blood. The samples were kept at RT for 10 minutes before being stored at -80°C until analysis. Upon analysis, these samples were quickly thawed at +37°C for 2 minutes, followed by a 15-minute incubation with fixing solution (Cytodelics AB) at RT. RBCs were then lysed in lysing buffer (Cytodelics AB) for 15 minutes at RT. The supernatant was removed by centrifugation at 300g for 10 minutes at RT. Cells were washed twice with wash buffer (Cytodelics AB) and flow cytometry staining buffer subsequently.

3.4.2. Proteomic stabilisers (Smart tubes, CA, US)

Blood samples were incubated in proteomic stabiliser (PROT1) solution for 10 minutes at RT and transferred to a -80°C freezer for storage. Samples were thawed in a +10°C water bath. RBCs were lysed by incubating samples in 1x thaw-lyse buffer (Smart tubes Inc) for 10 minutes at RT. Cells were collected after centrifugation at 600g for 5 minutes at RT. RBC lysis was repeated one more time before processing to staining.

3.4.3. Stable lyse – stable store V2 reagent (Smart tubes, CA, US)

Blood samples were added to Stable Lyse solution (Smart tubes Inc) and incubated at RT for 15 minutes. Subsequently, Stable Store solution (Smart tubes Inc) was added, and the samples were kept at RT for another 15 minutes before being stored at -80°C. Upon analysis, samples were thawed in a +10°C water bath and washed twice with staining buffer before staining.

3.4.4. Bulk Transfix (Cytomark, UK)

0.1ml bulk transfix solution was added to 0.5ml of blood samples, followed by a 15-minute incubation at RT. Samples were kept at +4°C for a maximum of 2 weeks before analysis. Before using, samples were kept at RT for 15 minutes. The cells were resuspended thoroughly and transferred to FACS tubes before continuing with a stain-lyse-wash procedure. After fluorochrome-conjugated monoclonal antibody mixture was added,

samples were incubated in dark at RT for 25 minutes. Afterwards, samples were subjected to 1x BD FACS™ lysing solution (BD Biosciences),

3.4.5. Peripheral Blood Mononuclear Cell Isolation and freezing

Blood was diluted with phosphate buffered saline solution (PBS) (1:3) before being layered on top of Ficoll® Paque Plus (GE Healthcare, USA). The ratio of blood to Ficoll followed the manufacturer's recommendation. Samples were then centrifuged at 400g for 30 minutes at RT without break. After the centrifugation, PBMCs were collected from the cloudy layer above Ficoll, followed by two washes with PBS.

In a cryotube, 500ul CTL-Cryo™ C Media (ImmunoSpot, USA) was added to 5-10 million PBMCs. CTL-Cryo™ AB Media was mixed before using and kept at 37^{o}C. CTL-Cryo™ AB is added to the cryotube containing PBMC by dropwise over 2 minutes on a low-speed vortex. The mixture was immediately placed into Mr Frosty™ Freezing Container (Thermo Scientific^{TM}, USA) or a CoolCell controlled-rate freezing container (BioCision, USA) and moved to -80°C freezers

Upon thawing, samples were placed in a +37^{o}C water bath for 2 minutes. All medium from each cryovial was transferred to a 50ml conical tube. To yield high cell viability, the first 3ml of thawing media (90% RPMI, 10% CTL wash, 10ug/ml DNase) was added slowly while gently swirling the tube, followed by adding another 7ml of thawing media at an average speed. Samples were centrifuged at 330g for 10 minutes, and the supernatant was removed. The process was repeated twice to remove all DMSO and preservative reagents.

3.5. Granulocyte activation

Whole blood was stimulated with 5ug/ml LPS or 100umol/ml for 1 hour in a +37°C incubator with 5% CO_2. The reaction was stopped and washed with cold PBS. Cells were then centrifuged at 330g for 10 minutes. The cell pellet was reconstituted in PBS and processed further with either BD FACS lysing for immediate analysis or stored in different cryopreservation reagents for later use.

3.6. Flow cytometry

3.6.1. Panel design

First, populations of interest were defined. The expression density of each marker and co-expression were then assessed. The information was combined with data from a resolution impact matrix to minimise spectral spillover and loss of resolution. In general, dim fluorochromes were assigned to well-defined and highly expressed proteins and vice versa. Two co-expressed proteins were put into no or very few overlapping channels. How these conditions were addressed was also dependent on flow cytometers and the availability of antibodies. However, the resolution of target populations was maximised to the best extent. The designing process was aided by BD Horizon™ Guided Panel Solution tool[84].

3.6.2. Compensation

Compensation was used to correct for the fluorescence spillover. Compensation matrices were established from single staining files using CompBead Ig, κ/Negative Control Particles Set (BD Biosciences). Used antibodies were similar to corresponding panels (Table 3Table 3: Fluorescence–labelled antibodies used in each panel). To ensure the accurate positive signal of dim populations, photomultiplier tube (PMT) voltage of each channel was set so that the robust standard deviation (rSD) of the negative population was placed at 2.5xrSD of the electronic noise. Later, compensation matrices were generated automatically in Flowjo software and applied to the acquired flow cytometric data

3.6.3. Staining and acquisition

Prior to the staining, all antibodies were titrated using Cytodelics-preserved samples. The final antibody concentration was selected based on the highest separation index[85].

$$\text{Separation Index} = \frac{\text{MedianPositive} - \text{MedianNegative}}{(84\%\text{Negative} - \text{MedianNegative})/0.995}$$

Monitoring of flow cytometer performance was performed at each cold start. The instrument was left on for 20 to 30 minutes to warm up and standardize lasers. Then Cytometer Set-Up and Tracking (CST) beads (BD Biosciences, USA) was run to track the

instrument performance and any deviation from the baseline. Samples were acquired only when all parameters passed the CST test.

All staining was done in dark at +4°C. One to five million cells were first suspended in Brilliant Stain Buffer (BD Bioscience, USA). In some experiments, samples were first treated with 2.5µg Human BD Fc Block™ (BD Biosciences) or 100U/ml Heparin (Sigma-Aldrich, USA) for 20 minutes. Subsequently, an antibody cocktail for surface markers was added, followed by a 30-minute incubation. If needed, the samples were then washed with 1X permeabilisation buffer (eBioscience, USA), followed by staining with antibodies for intracellular markers for 30 minutes in dark at 4°C. After washing twice with FACS staining buffer (PBS with 2% FCS and 2mM EDTA), they were ready for acquisition in LSRII Fortessa (BD Biosciences, USA). About 120 000 to 250 000 cells were recorded for studying the whole blood stabilisers, and about 1 to 1.5 million cells were recorded for the COVID-19 experiments.

Table 3: Fluorescence–labelled antibodies used in each panel

Fluorochrome	Antigen	Clone	Host	Cat number	Manufacturer
Panel for immune cell lineages					
PE	HLA-DR	MEM-12	Mouse	21278994	ImmunoTools
PE-CF594	CD8	RPA-T8	Mouse	562282	BD Biosciences
PerCP-Cy5.5	CD14	M5E2	Mouse	550787	BD Biosciences
APC	CD3	HIT3b	Mouse	21810036	ImmunoTools
APC-R700	CD56	NCAM16.2	Mouse	565140	BD Biosciences
APC-H7	CD45	2D1	Mouse	560274	BD Biosciences
BV421	CD4	RPA-T4	Mouse	562424	BD Biosciences
BV510	CD15	W6D3	Mouse	563141	BD Biosciences
BV605	CD19	HIB19	Mouse	302244	BioLegend
BV786	CD16	3G8	Mouse	563690	BD Biosciences
Panel for granulocyte activation					
FITC	CD19	HI19a	Mouse	21810193	ImmunoTools
FITC	CD56	MEM-188	Mouse	21270563	ImmunoTools
FITC	CD14	18D11	Mouse	21620143	ImmunoTools
FITC	CD3	HIT3b	Mouse	21810033	ImmunoTools
PE-Cy7	CD66b	G10F5	Mouse	25066642	Invitrogen
Per-CP cy5.5	CD69	FN50	Mouse	560738	BD Biosciences
APC	siglec8	7C9	Mouse	347105	biolegend

Fluorochrome	Antigen	Clone	Host	Cat number	Manufacturer
AF780	CD62L	DREG-56	Mouse	47-0629-42	eBioscience
BV421	CD45	HI30	Mouse	563880	BD Biosciences
BV510	CD15	W6D3	Mouse	563141	BD Biosciences
BV605	Cd11b	ICRF44	Mouse	562723	BD Biosciences
BV786	CD16	3G8	Mouse	563690	BD Biosciences
Panel for T lymphocytes					
FITC	CD19	HI19a	Mouse	21810193	Immunotools
FITC	CD14	18D11	Mouse	21620143	Immunotools
PE-CF594	CCR7 (CD197)	150503	Mouse	562381	BD Biosciences
Pe-Cy7	CD31	WM59	Mouse	563651	BD Biosciences
Alexa Fluor 700	CD3	UCHT1	Mouse	557943	BD Biosciences
BV421	CD95 (FAS)	DX2	Mouse	562616	BD Biosciences
BV510	CD4	SK3	Mouse	562970	BD Biosciences
BV605	TCRgd	B1	Mouse	740415	BD Biosciences
BV650	CD8	SK1	Mouse	344730	Biolegend
BV711	CD45RA	HI100	Mouse	563733	BD Biosciences
Panel for Neutrophils in COVID-19					
FITC	CD19	HI19a	Mouse	21810193	ImmunoTools
PE	CD33	WM53	Mouse	555450	BD Biosciences
PE-Cy7	Ki-67	B56	Mouse	561283	BD Biosciences
Per-CP cy5.5	HLA-DR	L243	Mouse	552764	BD Biosciences
APC	ARG1	14D2C43	Mouse	369706	Biolegend
Alexa Flour 700	CD3	UCHT1	Mouse	557943	BD Biosciences
APC-Cy7	CD11b	M1/70	Rat	101226	Biolegend
BV421	Lox-1	NA	Mouse	358610	Biolegend
BV510	CD15	W6D3	Mouse	563141	BD Biosciences
BV605	CD16	3G8	Mouse	563173	BD Biosciences
BV711	CD274 (B7-H1)	29E.2A3	Mouse	329721	Biolegend
BV786	CD14	M5E2	Mouse	563698	BD Biosciences

3.7. Analysis

The obtained flow cytometry data were analysed with Flowjo software (v10.7.1, BD Bioscience, USA). The sample median values in matched materials were compared by statistical tests for non-parametric data as indicated in each figure. The statistical analysis and graph design were performed using Prism 9 (GraphPad Software Inc, USA). A P-value smaller than 0.05 was considered statistically significant.

High-dimensional data analysis of flow cytometry data

Uniform Manifold Approximation and Projection (UMAP) and Self-Organising Maps (FlowSOM) clustering was performed on the Flowjo software. All FCS files were preprocessed to correct for spectral spillover and remove debris, singlets, eosinophils and B cells. An equal sampling of 10000 events from each FCS file was done using DownSample plugin in Flowjo, which were then concatenated into a single flow cytometry file of 280 000 cells. The following markers were used for FlowSOM and UMAP analysis: CD3, CD15, CD16, CD14, HLA-DR, CD11b, CD33, CD274 (PD-L1), ARG1, LOX-1, Ki-67. All cells were projected on UMAP's two-dimensional space. UMAP plots were generated with Euclidean distance, 10 for nearest neighbor, 0.5 for minimum distance and 2 for total components. Resulting UMAP plots were fed into the FlowSOM clustering algorithm (number of cluster=13)[86].

4. Results

4.1. **Optimisation of whole blood stabilisers**

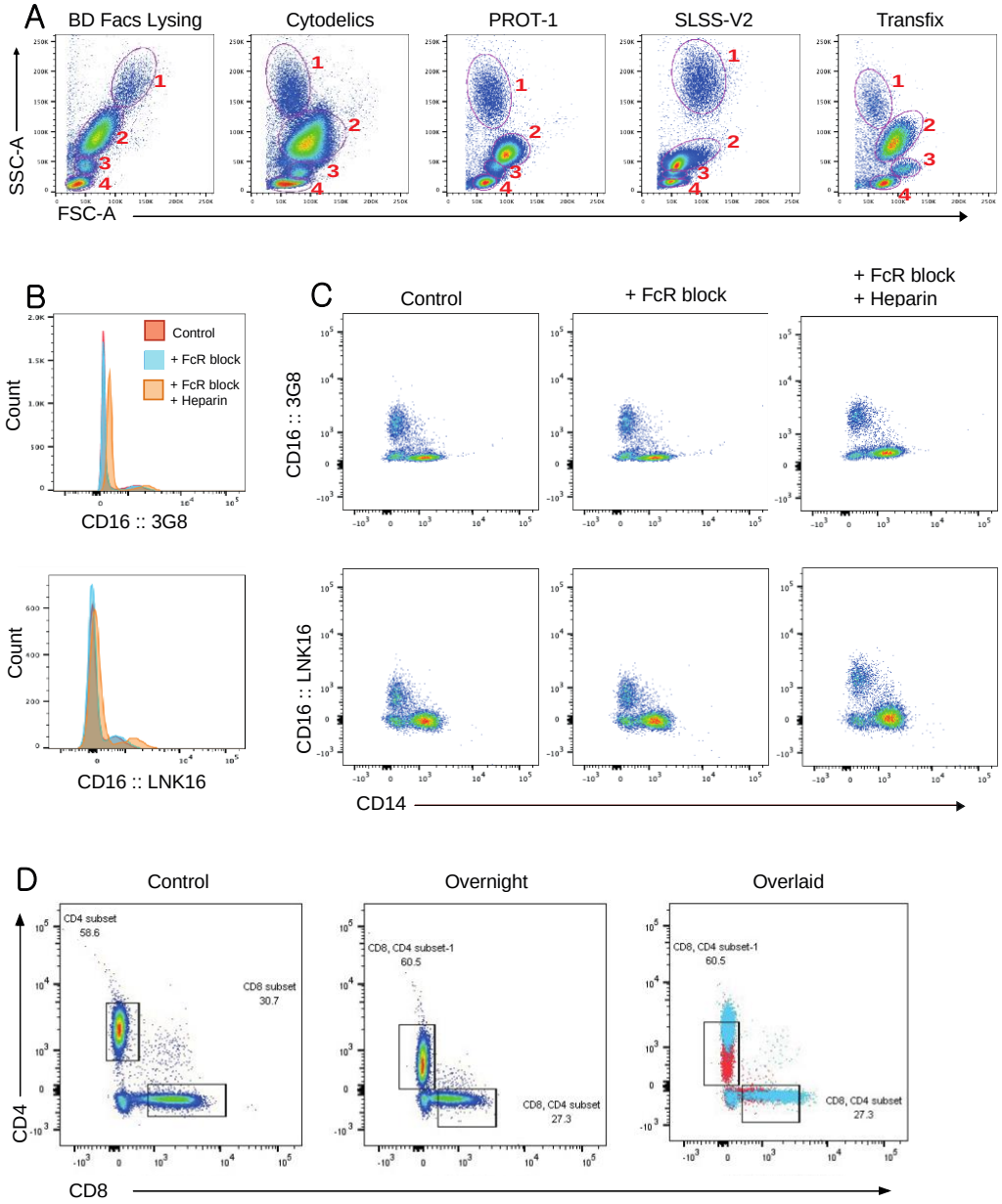

Figure 6: Overview of stabiliser effects. (A) Representative FSC/SSC profile of the same donor resulted from each stabiliser. (1) Eosinophils; (2) Neutrophils; (3) Monocytes; (4) Lymphocytes. Note that FSC files of each stabiliser were recorded at different FSC/SSC voltages to capture all the events. (B)(C) Effects of clones, FcR block, and 100U/ml heparin on CD16 staining of samples preserved in Cytodelics (n=2). (D) Samples preserved in Cytodelics stained immediately (control) and 24h after thawing (overnight).

Samples treated with BD FACS Lysing solution were considered as fresh and unpreserved control in our study. A stain-lyse-wash procedure was used to minimize the effects of fixation and permeabilization on antibody staining. Our preliminary data showed that BD FACS Lysing Solution lysed RBCs and maintained distribution of major immune sup-population equivalent to samples traditionally processed with Ammonium-Chloride-Potassium (ACK) lysis buffer (data not shown). Furthermore, according to Euroflow standardization published on Nature Leukemia, BD FACS Lysing solution also yielded the best discrimination between major immune cell populations and the highest fluorescence intensity values with a minimal cell loss compared to other erythrocyte lysing solutions[87]. BD FACS lysis solution was also certified as an in-vitro diagnostic (IVD) product which is often ensured with a high level of safety and efficacy. Similarly, Transfix – another IVD reagent, was expected to have a high performance for cryo-preservation, so in some analyses, we used it as a second control of fixed samples, which resembles whole blood stabilisers more than the unpreserved control.

Whole blood stabilisers under investigation were Cytodelics, Proteomic stabiliser (PROT-1), Stable lyse stable store V2 (SSLS-V2) and Transfix. All stabilisers changed forward scatter/side scatter (FSC/SSC) compared to the fresh control within an acceptable range, and each stabiliser's FSC/SSC profile was slightly different from each other (data not shown). This issue was expected since fixation with formaldehyde and low temperature were shown to alter cell morphology[25]. Compared to the fresh sample, eosinophils in cryopreserved samples showed the most apparent change in size, indicated by a shift to the right on the FSC axis (Figure 6).

However, by adjusting acquisition voltages of FSC and SSC, it was possible to distinguish distinct populations of lymphocytes, monocytes, and granulocytes in all stabilisers except SLSS-V2 (Figure 6). Nevertheless, the overlap between monocytes and neutrophils in SLSS-V2 could possibly be corrected to some extent by using specific markers such as CD14 and CD15, respectively (Figure 8).

Some markers in samples preserved in Cytodelics were sensitive to antibody staining. For example, it was challenging to separate positive and negative populations using anti-human CD16 antibody with LNK16 clone alone (Figure 6B & C). 2.5ug FcR blocking reagent and 100U/ml heparin were used to reduce unspecific staining. Though FcR blocker alone did

not show any effect, its combination with heparin was more effective to distinguish between different populations. However, antibody clone was more crucial to the staining quality. Both histogram and the FCS plot of CD16 staining with the 3G8 clone showed a more apparent separation between negative and positive events than the LNK16 clone. It was sufficient to distinguish the two populations even without FcR blocker or heparin (Figure 6B & C). It was, therefore, essential to test and verify antibody clones before staining for samples stabilised in Cytodelics. From our experience, the other stabilisers did not show such a strict preference for antibody clones as Cytodelics.

It was equally important to do the antibody staining right after thawing of samples cryopreserved in Cytodelics. For example, after 24 hours, the fluorescence intensity of both CD4 and CD8 reduced. Positive and negative populations became overlapping (Figure 6D). Processing right after thawing was also reported to be essential for PROT-1 since blood samples could form clumps and change color otherwise [88].

4.2. Detection of lineage subsets

Samples treated with BD Facs lysing had major leukocyte lineages easily identified, as shown in the gating strategy in Figure 7A. As a common leukocyte marker, total CD45 expression was used as an indicator of total leukocytes. The other stabilisers displayed a similar pattern across all four donors. Median fluorescence intensity (MFI) of some lineage markers such as CD3, CD19, CD56, and CD14 seemed to be comparable between long-term cryo-preserved reagents – Cytodelics, PROT-1, and SLSS-V2. However, these MFI values were quite different in samples treated with BD Facs Lysing and Transfix. For example, these two had CD19 signals almost twice as intense as the level of samples cryopreserved in the other stabilisers. The reverse trend applied for CD56 MFI (Figure 8A). Therefore, it was impossible to make a fair comparison between all the conditions based on non-normalised MFI values.

Our flow cytometry panel allowed the discrimination of major $CD45^+$ immune subsets. The frequency of $CD15^+$ granulocytes was comparable between controls and preserved samples, whereas the distribution of monocyte subsets could not be correctly identified due to the signal reduction in CD14. Though experiencing a partial loss of signal, Cytodelics and PROT-1 treated samples had CD14 negative and positive events separately clearly. The

separation was almost completely abolished in SLSS-V2 and Transfix fixed samples. (Figure 7B)

Loss of CD14 signal resulted in a significant decrease in the frequency of classical ($CD14^{+}CD16^{-}$) and intermediate ($CD14^{+}CD16^{+}$) monocytes in all preserved samples (Figure 8C). Among all stabilisers, Cytodelics had the best performance, detecting 80% of classical monocytes on average, whereas SLSS-V2 showed the worst outcome. One reason could be the overlapping between monocyte and neutrophil on SSC/FSC plots of SLSS-V2 samples, making the initial gating to separate them inaccurate (Figure 6A and Figure 7A).On the other hand, non-classical monocytes ($CD14^{-}CD16^{+}$) increased slightly in all preserved samples. Cytodelics, however, kept that increase modest and comparable to Transfix, the IVD product. (Figure 8C)

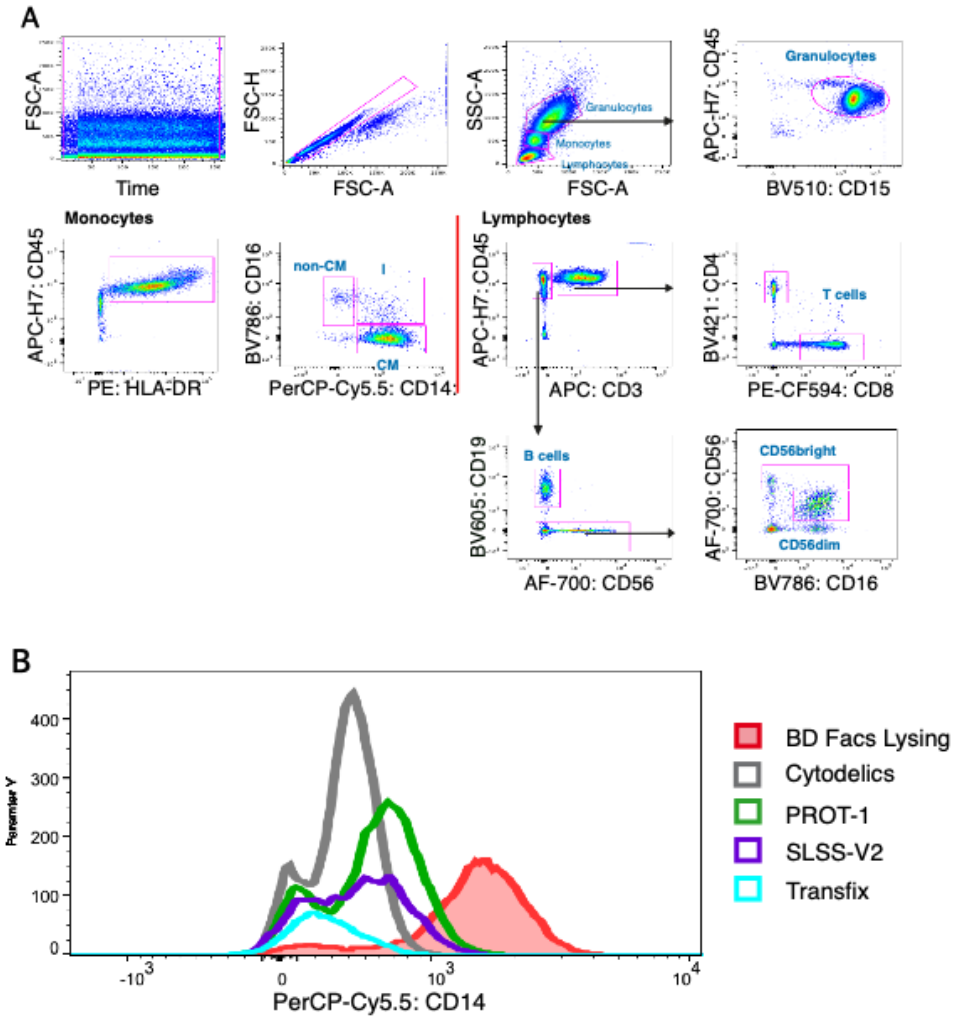

Figure 7: Detection of major lineage subsets. (A) Representative flow cytometry plots of the gating strategy. (B) Representative histogram of CD14 expression (n=4). Non-CM, non-classical monocytes; I, intermediate monocyte; CM, classical monocyte.

All stabilisers preserved lymphocytes reliably. Our focus was dim ($CD56^{+}CD16^{+}$) and bright ($CD56^{++}CD16^{low/-}$) NK cells, T cells ($CD3^{+}CD4^{+}$ or $CD3^{+}CD8^{+}$) and B cells ($CD19^{+}$). The frequency of all these subsets was detected in both unpreserved and preserved samples without statistical differences. Though existing, the differences were minor, accounting for less than 10%). In general, Cytodelics and PROT-1 were the most robust in detecting highly expressed immune lineages, particularly for lymphocytes. (Figure 8D-F)

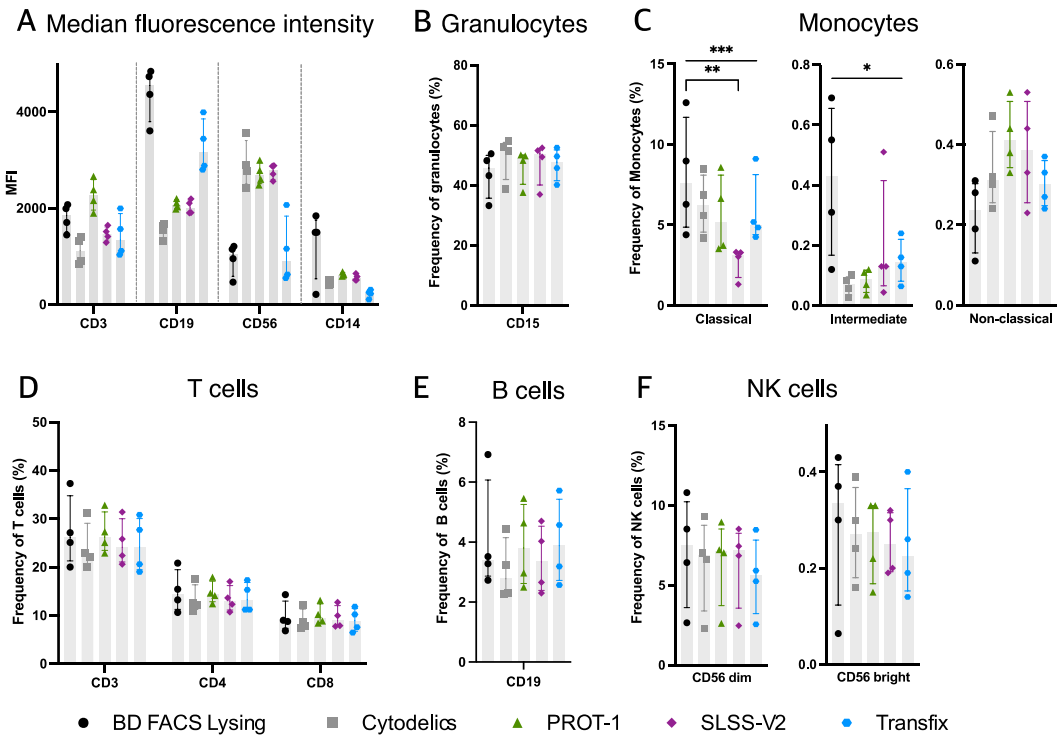

Figure 8: Distribution of lineage subsets depending on types of markers and stabilisers. (A-F) Percentage of each lineage subsets within total $CD45^{+}$ single cells, (A) granulocytes; (B) Monocytes; (C) T cells; (D) B cells; (F) Natural killer (NK) cells. All graphs showed median values with interquartile range (n=4). Black circle – BD FACS Lysing; grey square – Cytodelics; green triangle – PROT-1, purple octahedron – SLSS-V2; blue hexagon – transfix. Statistical analysis was done with the Friedman test for nonparametric data. *,$p \leq 0.05$; **,$p \leq 0.01$; ***,$p \leq 0.001$.

4.3. Detection of T cell subsets

As the frequency of major T cells markers – CD3, CD4, and CD8, were quite similar between the stabilisers and controls (Figure 8D), we investigated further how these reagents preserve different subsets of T lymphocytes. Here we optimised the staining for surface markers to distinguish between gamma delta ($TCR\gamma\delta^{+}$); naïve ($CCR7^{+}CD45^{+}$), effector memory

($CCR7^{-}CD45^{-}$), central memory ($CCR7^{+}CD45^{-}$), TEMRA ($CCR7^{-}CD45^{+}$) and recent thymic emigrant (RTE) ($CCR7^{+}CD45^{+}CD31^{+}CD95^{-}$) T cells.

Both the fresh control (treated with BD FACS lysing) and commonly used cell fraction, peripheral blood mononuclear cells (PBMCs) exhibited comparable frequency of $TCR\gamma\delta^{+}$, naïve, and memory T cells (Figure 9C and Figure 10A & B). Since the nature of the fresh control and PBMC was very different – whole blood with formaldehyde fixation and a fraction of blood with cryopreservation, it was expected to have a slight variation. In other words, the fresh control was reliable to study circulating T cell subgroups.

The frequency of γδ T cells was variable between the fresh and cryo-preserved samples. There was also a two-fold reduction of this population in Transfix treated samples compared to the fresh control. The decline was even more severe in Cytodelics, PROT-1, and SLSS-V2, where the observed change was almost 3-fold (Figure 9C). This was due to the loss of TCRγδ signal resolution in these stabilisers (Figure 9B). Interesting, the detection was quite similar between these stabilisers, as observed in all four donors. This finding suggests that cryopreservation at a very low temperature (-80^{o}C) may interfere with the structure of TCRγδ. In general, it was not optimal to assess γδ T cell frequency in whole blood after cryopreservation.

Table 4: Markers to identify different circulating subpopulations of CD4 and CD8 T cells

	CD45RA	*CCR7*	*CD31*
Naïve	+	+	+/–
Central Memory	–	+	NA
Effector memory	–	–	NA
TEMRA	+	–	NA
Recent thymic emigrants	+	+	+ (*)

NA: not available or non-relevant.
**: only for CD4 T cells*

Naïve and memory subsets of both CD4 and CD8 were detected based on expression of CD45RA and CCR7 (Table 4). Contrary to the expectation for an IVD graded reagent, Transfix maintained CCR7 signal poorly, as did also all other whole blood stabilisers. Transfix, Cytodelics, and PROT-1 treated samples showed far less positive CCR7 events than the unpreserved control. Though positive and negative population was distinguishable in CD8 fraction, the separation was absent in CD4 fractions (Figure 10C). The reduced signal intensity of CCR7 explained a loss of about 40 to 50% in $CD4^{+}$ naïve and central memory cells as well as

an increase in CD4⁺ effector memory population among samples treated with these three reagents (Figure 10A). The frequency of CD4⁺ RTEs was also widely different across all stabilisers since they were a subgroup of naïve cells.

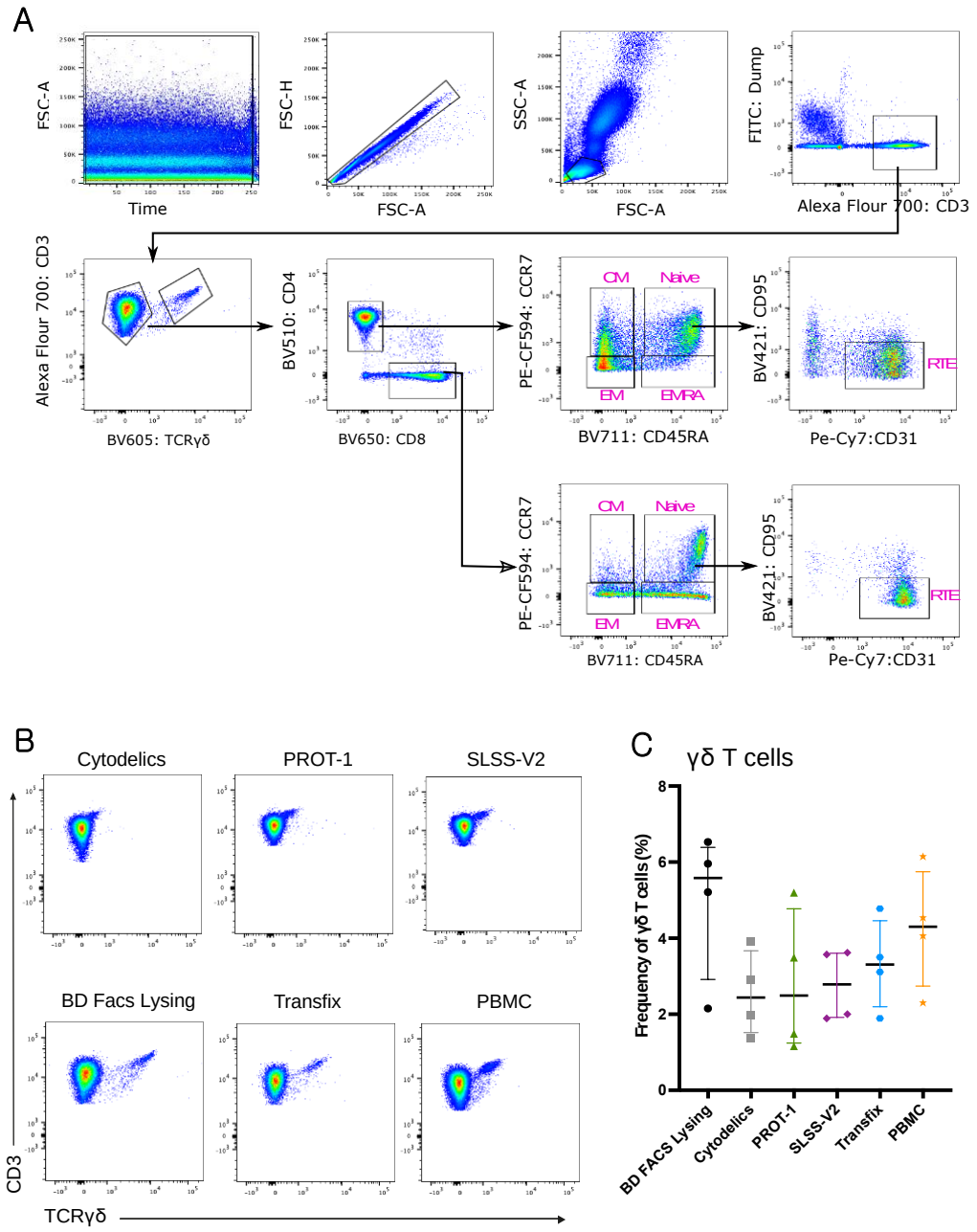

Figure 9: Cytodelics, PROT-1 and SLSS-V2 caused a reduction in the frequency of TCRγδ T cells. (A) Representative flow cytometry plots of the gating strategy for different T cell subsets. CM – central memory; EM – effector memory; EMRA – Terminally differentiated effector memory; RTE – Recent thymic emigrants. (B) Representative flow cytometry plots of TCRγδ expression (C) Frequency of γδ T-cells out of total CD3⁺ cells across stabilisers and PBMC. Black circle – BD FACS Lysing; grey square – Cytodelics; green triangle – PROT-1, purple octahedron – SLSS-V2; blue hexagon – Transfix; orange star – PBMC. Statistical analysis was done with the Friedman test for nonparametric data.

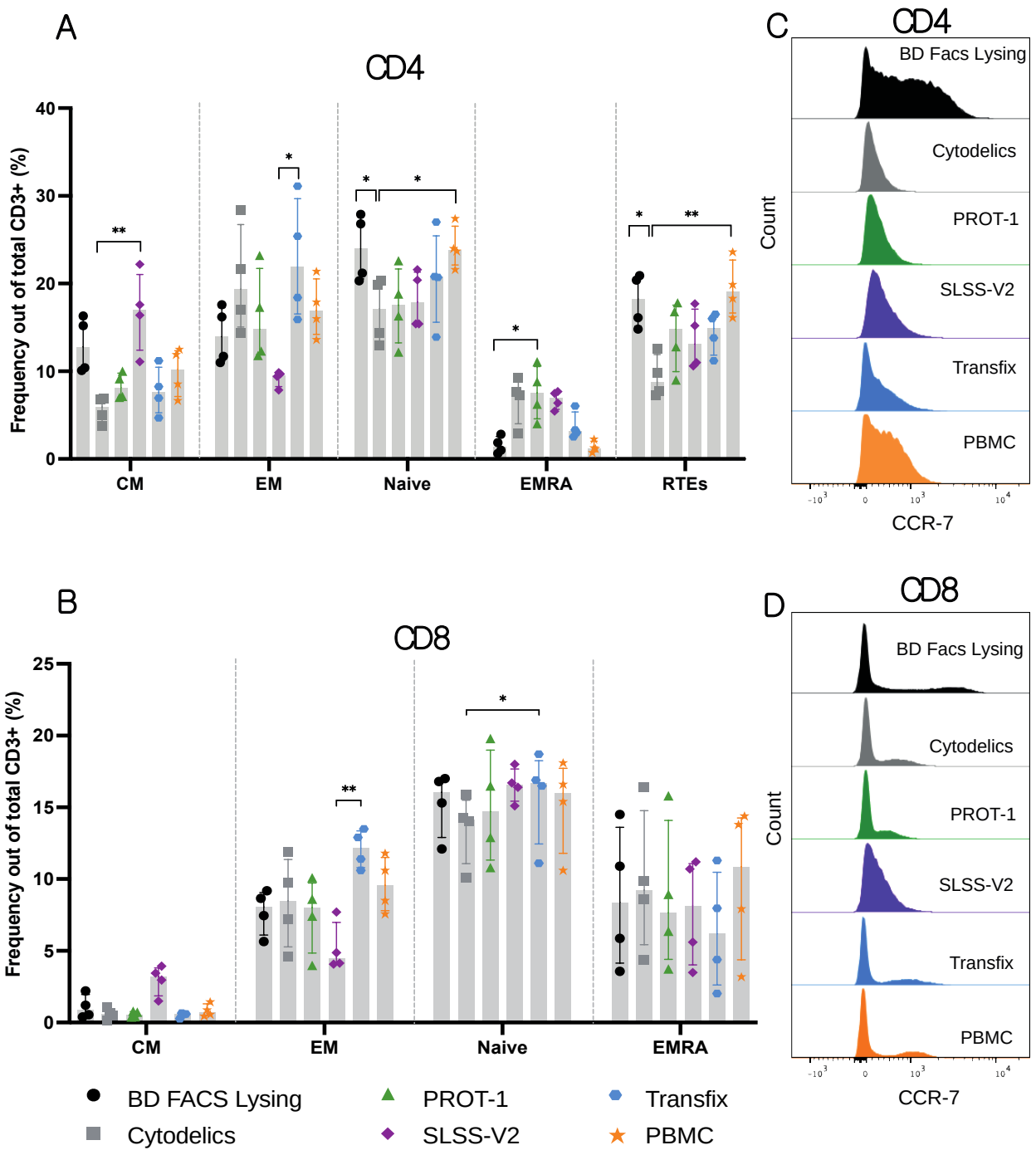

Figure 10: Detection of naïve and memory T cell subsets shifted significantly in Cytodelics, PROT-1 and SLSS-V2. (A) & (B) frequency of naïve and memory T cells out of total $CD3^+$ cells across different stabilisers. (C)& (D) representative histogram plots of CCR7 expression on CD4 and CD8 T cells (n=4). CM – central memory; EM – effector memory; EMRA – Terminally differentiated effector memory; RTE – Recent thymic emigrants. Black circle – BD FACS Lysing; grey square – Cytodelics; green triangle – PROT-1, purple octahedron – SLSS-V2; blue hexagon – Transfix; orange star – PBMC. Statistical analysis was done with the Friedman test for nonparametric data. *,$p \leq 0.05$; **,$p \leq 0.01$; ***,$p \leq 0.001$.

Since the CCR7 signal was better among $CD8^+$ cells, the frequency of CD8 subsets was more comparable between the fresh control and samples stabilised in Cytodelics and PROT-1. Notably, the quantification of naïve, EMRA, CM and EM subsets in Cytodelics and RPOT-1 were comparable to the control and PBMC. Besides, Transfix performed well in detecting naïve T cells but poorly for EM and EMRA subsets. In addition, SLSS-V2 was the least reliable reagent for phenotyping T cell subsets as there were no clear CCR7 positive events in both CD4 and CD8 fractions. In other words, all whole blood preserving reagents studied here maintained chemokine receptor – CCR7 staining intensity poorly.

4.4. Detection of granulocyte activation markers

One of the most significant advantages of whole blood cryopreservation and fixation is that cellular structure and integrity could be preserved right after blood drawing, reducing variation introduced by logistics and sample processing. If the method works, it will be ideal for studying granulocytes since they are short-lived and easily activated cells. In this study, we stimulated whole blood samples with LPS and fMLP for one hour at $+37^oC$ and then accessed granulocyte markers and their changes in expression in both pre-and post-cryopreservation.

LPS and fMLP stimulation resulted in a significant shift in the expression level of granulocyte activation markers in fresh controls (Figure 11B). Upon stimulation, both eosinophils and neutrophils were observed to have down-regulation of CD62L and up-regulation of CD11b, CD16, and CD66b (Figure 11C). Specifically, neutrophils had CD62L MFI reduced by 65% on average, whereas CD11b and CD66b expression increased by more than 100% compared to the control. On the other hand, CD16 had a modest change, only by a 20-30% increase. Compared to fMLP, LPS stimulated the expression CD62L and CD11b more (Figure 11D). Although a starting volume of blood was the same between conditions, a significant reduction in cell count after the stimulation was observed in fMLP-treated samples (Figure 11B). Many cells might have died during the incubation. Not only reducing viability, but fMLP also had drastically changed the size and granularity of granulocytes (data not shown).

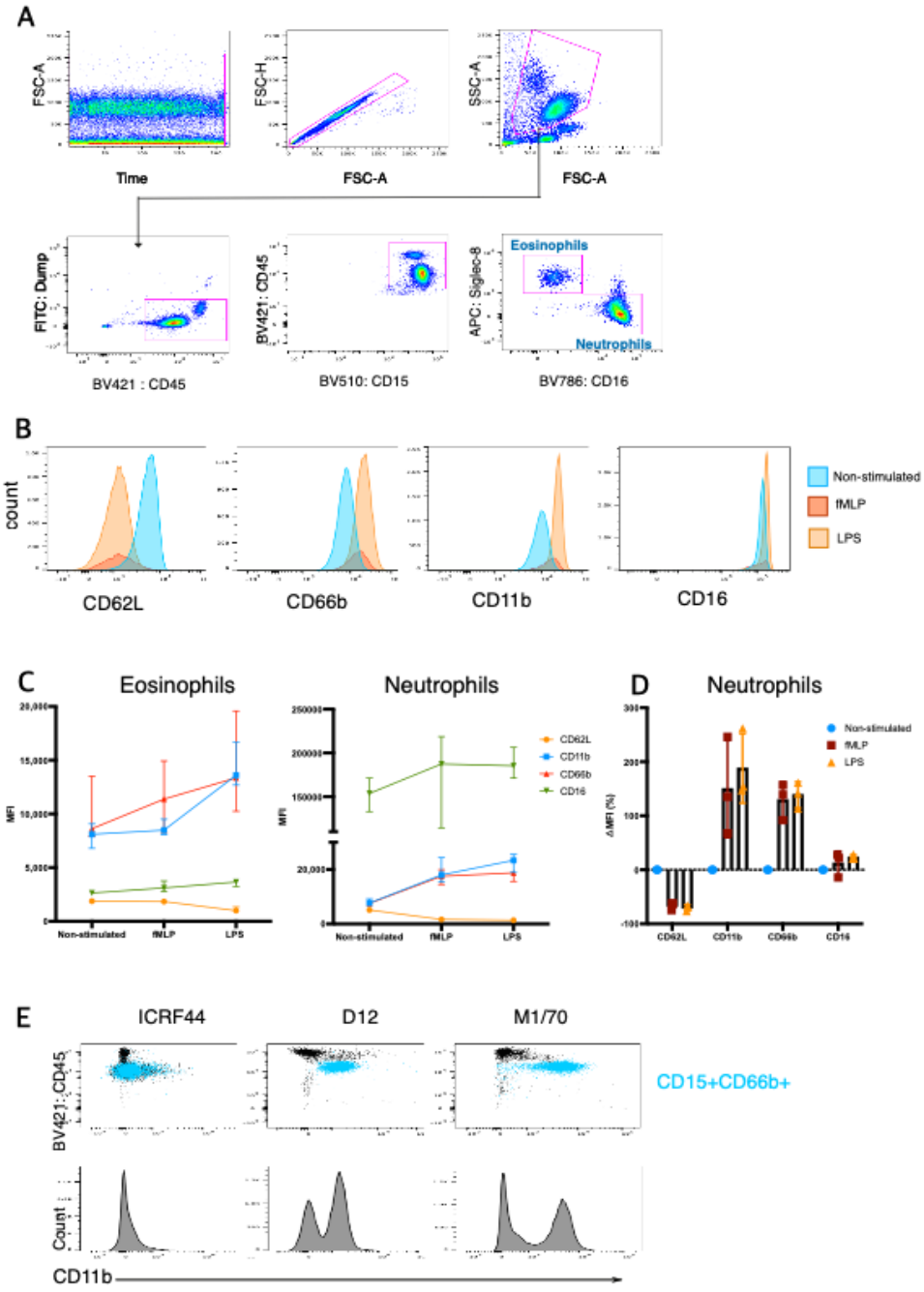

Figure 11: N-Formylmethionyl-leucyl-phenylalanine (fMLP) and Lipopolysaccharides (LPS) activated granulocytes. (A) Representative flow cytometry plots of the gating strategy to identify sub-population within granulocytes - eosinophils ($CD14^-$ $CD19^-$ $CD56^-$ $CD3^-$ $CD15^+$ $CD16^-$ $Siglec\text{-}8^+$) and neutrophils ($CD14^-$ $CD19^-$ $CD56^-$ $CD3^-$ $CD15^+$ $CD16^+$ $Siglec\text{-}8^-$). (B-D) Changes in granulocyte activation markers of fresh control upon LPS/ fMLP stimulation (n=3). (B) Representative histograms of these markers in neutrophils. (C) Median fluorescence intensity (MFI) in eosinophils and neutrophils. (D) Percentage of change in MFI of these markers in neutrophils. Data were normalised using unstimulated samples. The frequency below 0 indicates the percentage of reduction. (E) CD11b detection in samples treated with Cytodelics using different antibody clones (ICRF44, D12, and M1/70). Blue area indicated $CD15^+$ $CD66b^+$ granulocyte population where CD11b was often found to be co-localised.

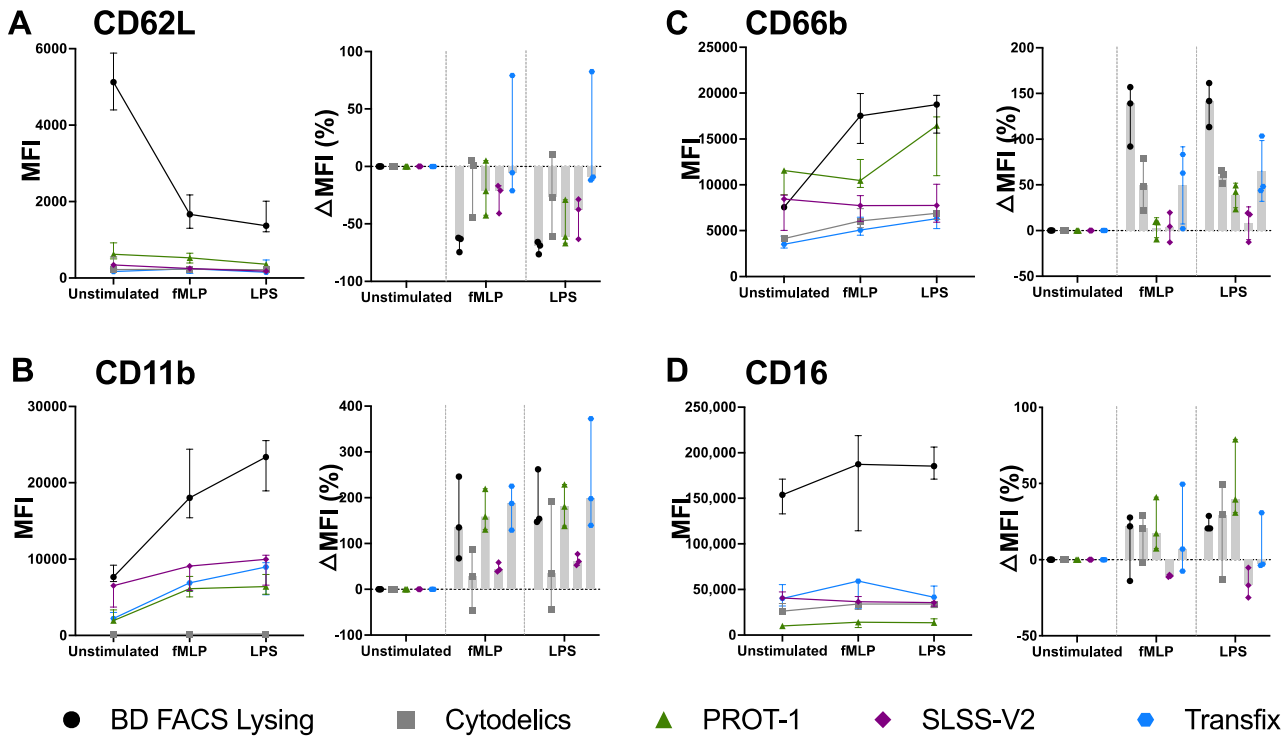

Figure 12: Granulocyte activation status were maintained but signal intensity of indicated markers varied across the stabilisers. Data was shown in Median fluorescence intensity (MFI) and percentage of change in MFI for CD62L (A), CD11b (B), CD66b (C), CD16(D). (Median with range, n=3). The frequency below 0 indicates the percentage of reduction. Black circle - BD FACS Lysing; grey square - Cytodelics; green triangle - PROT-1, purple octahedron - SLSS-V2; blue hexagon – Transfix.

All whole blood stabilisers preserved the cellular activation immunophenotype after stimulation with fMLP and LPS to some extent, even though activation markers were detected at much lower MFI than the fresh control one. Among them, PROT-1 stood out the most in terms of performance. It allowed the best detection of the expressional trend of activation markers such as CD62L, CD11b, and CD16 upon the activation with both fMLP and LPS (Figure 12). Though there was almost no change in CD66b expression upon fMLP stimulation in these samples, it was clearly elevated in LPS-stimulated ones. However, PROT-1 could not reflect all the degree of changes in CD66b expression since we could detect only about a 50 percent increase in CD66b in PROT-1-treated cells compared to more than 150 percent in the fresh controls. Similarly, all stabilisers caused a dramatic reduction in CD62 MFI and its proportion of MFI changes upon stimulation. Only PROT-1 retained the degree of CD62L decline after LPS stimulation comparable to the controls. (Figure 12).

The second-best performance was with Cytodelics, which preserved relatively well the expression of CD66b, CD16 in both fMLP and LPS treated samples and to some extent CD62L as well, but only after LPS treatment. Again, the MFI and percentage of MFI changes in CD62L and CD66b after both stimulations were much lower than in the control. Strikingly, CD11b signal was almost absent due to the antibody clone used, even though we used the ICRF44 clone that the manufacturer had validated. However, when using this clone, positive events were indistinguishable from negative ones (Figure 11E). The problem was mitigated by using D12 or M1-70 clones. Therefore, Cytodelics seems to sufficiently maintain cellular structures of the markers mentioned above to detect neutrophil activation markers.

Contrary to our expectations, Transfix performed poorly for half the markers studied here, CD62L and CD16. Measurement of CD11b and CD66b were similar to samples preserved in Cytodelics and PROT-1. On the other hand, SLSS-V2 produced the worst result that three out of four activation markers, CD11b, CD66b, and CD16, had either no change at all or even a reverse trend compared to the control (Figure 12B-D).

4.5. Immune profiling of COVID-19 patients

4.5.1. Unsupervised analysis of flow cytometry data

Next, we investigated whether COVID-19 patient samples cryopreserved in Cytodelics would be suitable for immunophenotyping by flow cytometry. Cytodelics was selected because it was good at preserving common immune lineages and neutrophil activation markers. In addition, Cytodelics also offered logistic advantages. Since it was developed and currently used for mass cytometry in Sweden, it allowed more collaboration between Sweden and our research consortium located in Finland.

To investigate immune signatures of SARS-COV-2 infection, we compared acute and convalescent phases of 14 COVID-19 patients. Aggregated flow cytometry data were clustered by Self-Organising Maps (FlowSOM) and visualised on Uniform Manifold Approximation and Projection (UMAP) (Figure 13). FlowSOM identified 13 meta clusters, which overlaid with UMAP map (Figure 13A&C). Based on the FlowSOM heatmap, cluster 12 was solely $CD3^+$ T cells, whereas Cluster 0 and 4 included $CD14^+$ monocytes. On the other hand, Clusters 1, 2, 3, 5, and 7 contain different subsets of $CD15^+$ neutrophils. These subsets

showed a clear differential expression of CD16, which is in line with neutrophil maturation states. Cluster 1 was completely negative for CD16, indicating the presence of immature cells. Clusters 2, 5, and 7 probably contain both immature ($CD33^{+}$ $CD16^{+}$) and mature neutrophils ($CD33^{-/+}$ $CD16^{+/++}$). The most interesting population was cluster 3, which was defined as $CD16^{++}$ $ARG1^{+}$ $LOX\text{-}1^{+}$ $Ki\text{-}67^{+}$. This cluster 3 probably contained suppressive neutrophils because ARG1 and LOX-1 are known to be up-regulated in suppressive neutrophils[37,89,90]. (Figure 13B and Figure 14A)

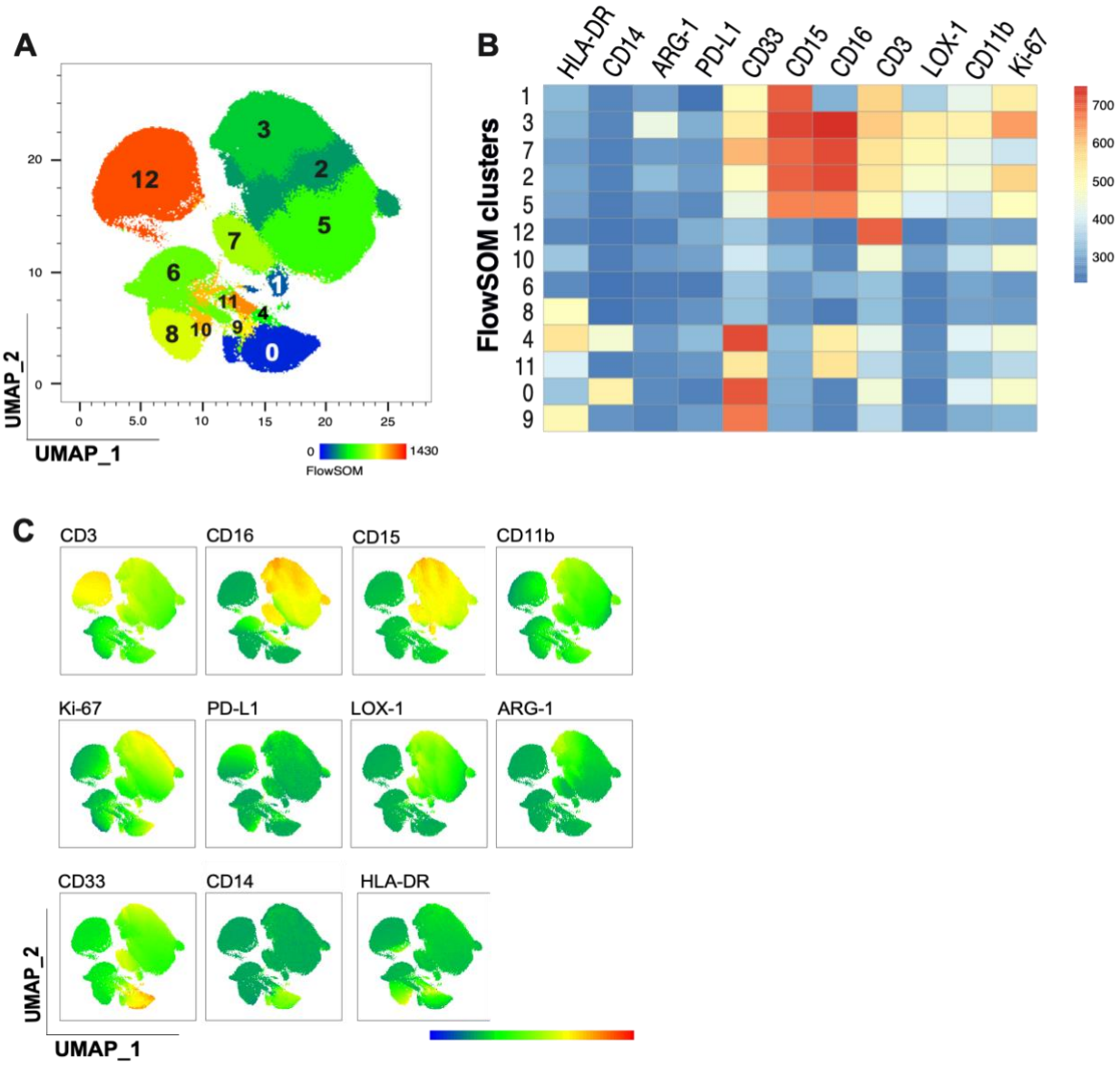

Figure 13: UMAP visualisation and FlowSOM clustering of concatenated flow cytometry data. Ten thousand cells were subsetted from each individual in a cohort of 28 COVID-19 patients. (A) UMAP visualisation of all individuals pooled with FlowSOM meta cluster overlaid. Colour and number indicate FlowSOM cluster-ID. (B) Heatmap of the FlowSOM meta clusters showing relative expression of indicated immune parameters. (C) UMAP projection of expression of the indicated proteins.

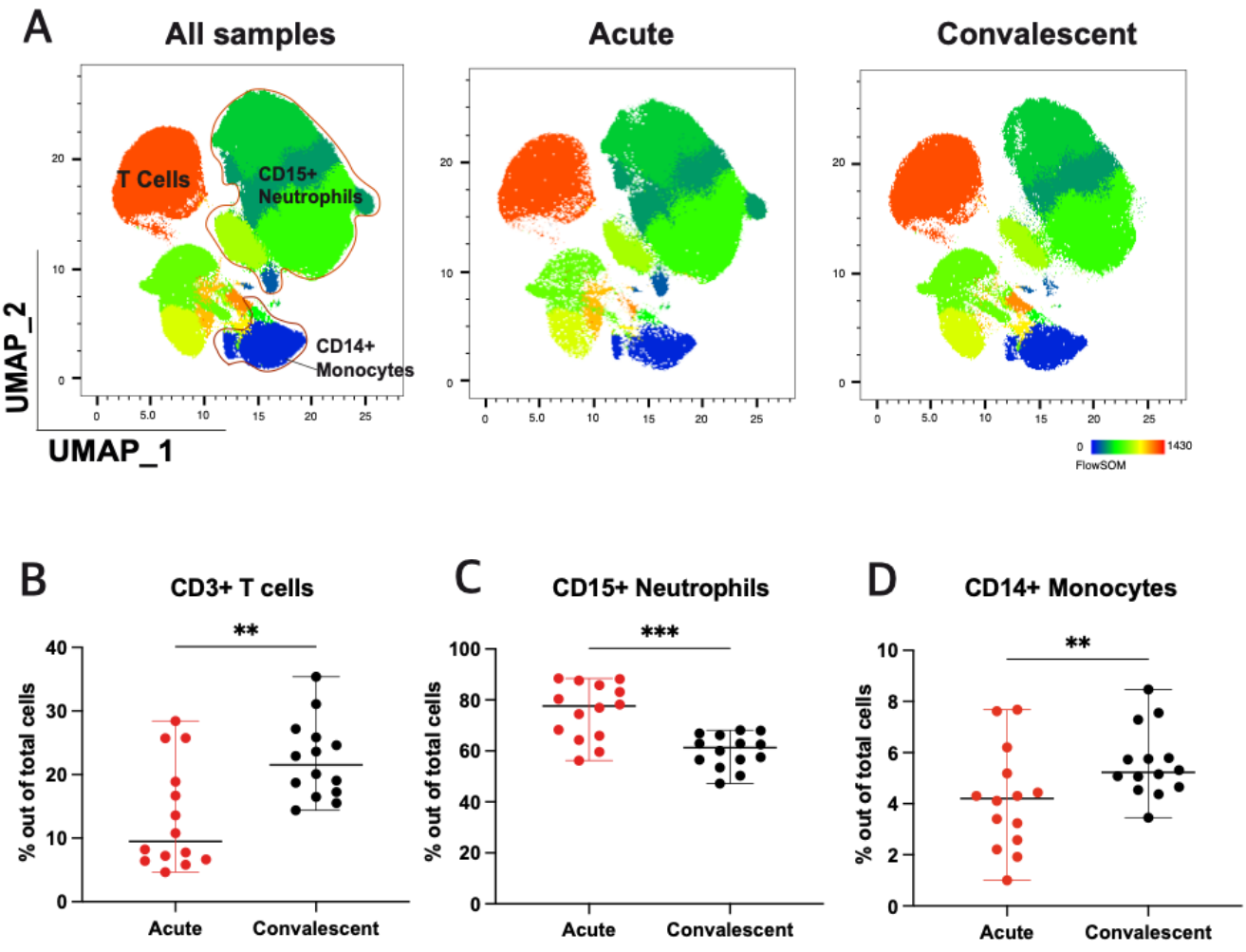

Figure 14: Cytodelics allowed reliable detection of highly expressed immune markers in COVID-19. A) UMAP projection of aggregated flow cytometry data all participants with FlowSOM meta cluster overlaid. (B) (C) (D) Percentages of CD3+ T cells, CD15+ Neutrophils and CD14+ Monocytes, respectively, among total cells. Statistical analysis was done with the Wilcoxon matched-pairs signed-rank test for nonparametric data. *,p ≤0.05; **,p ≤0.01; ***,p ≤0.001.

4.5.2. Longitudinal analysis of immune cell subsets in COVID-19

Next, we looked at the percentage of major lineage markers in each participant. The frequency of $CD3^+$ T cells decreased significantly in the acute compared to the convalescent samples, reflecting lymphopenia often seen in acute COVID-19. The T cell number increased almost two-fold after 90 days from symptoms onset. In addition, a similar reduction was observed in the frequency of $CD14^+$ monocytes, whereas the frequency of $CD15^+$ neutrophils elevated significantly during the acute phase.

4.5.3. Detection of neutrophil subsets in COVID-19 patients

As mentioned above, different subsets of neutrophils were identified by FlowSOM clustering, showing a separation of immature, mature, and activated cells based on CD16 expression (Figure 15A). Cluster 1 was entirely negative for CD16, indicating the presence of immature cells. These $CD16^{-}$ immature neutrophils increased significantly during the acute phase of the SARS-COV-2 infection. Acute samples of both the hospitalised and ICU groups displayed a similar elevation of $CD16^{-}$ without statistical differences. (Figure 15B)

According to FlowSOM, clusters 3, 2, 5, and 7 encompassed both immature ($CD33^{+}$ $CD16^{+}$) and mature neutrophils ($CD33^{-/+}$ $CD16^{+/++}$). Unfortunately, no statistical difference was detected between the acute and convalescent samples regarding these immature and mature neutrophil subsets. Moreover, there was no statistical difference between the acute and convalescent samples when the hospitalised and ICU groups were analysed separately . (Figure 15C – E)

Within the $CD16^{high}$ population, cluster 3 had a similar phenotype to suppressive neutrophils based on their expression of CD16, ARG1 and LOX-1. ARG1 and LOX-1 have been shown to be up-regulated in suppressive neutrophils[37,89,90]. However, we found no difference in frequency of these cluster 3 cells between acute and convalescent samples in either the hospitalised or ICU cohort. Surprisingly, this population accounted for 20 percent of total studied cells on average, which might indicate that other non-suppressive neutrophils can express LOX-1 and ARG1. Moreover, some patients had a very high number of these suppressive cells, up to 40% of total studied cells, whereas some patients had less than 5%. The phenomenon of dramatic differences in cluster 3 population between individuals was observed in both hospitalised and ICU cohorts. In addition, these suppressive-like cells were highly proliferative due to a high expression of Ki-67 compared to other subsets. In conclusion, we were unable to confirm if cluster 3 represented solely suppressive neutrophils or if it also contained other mature and activated neutrophils. (Figure 15E)

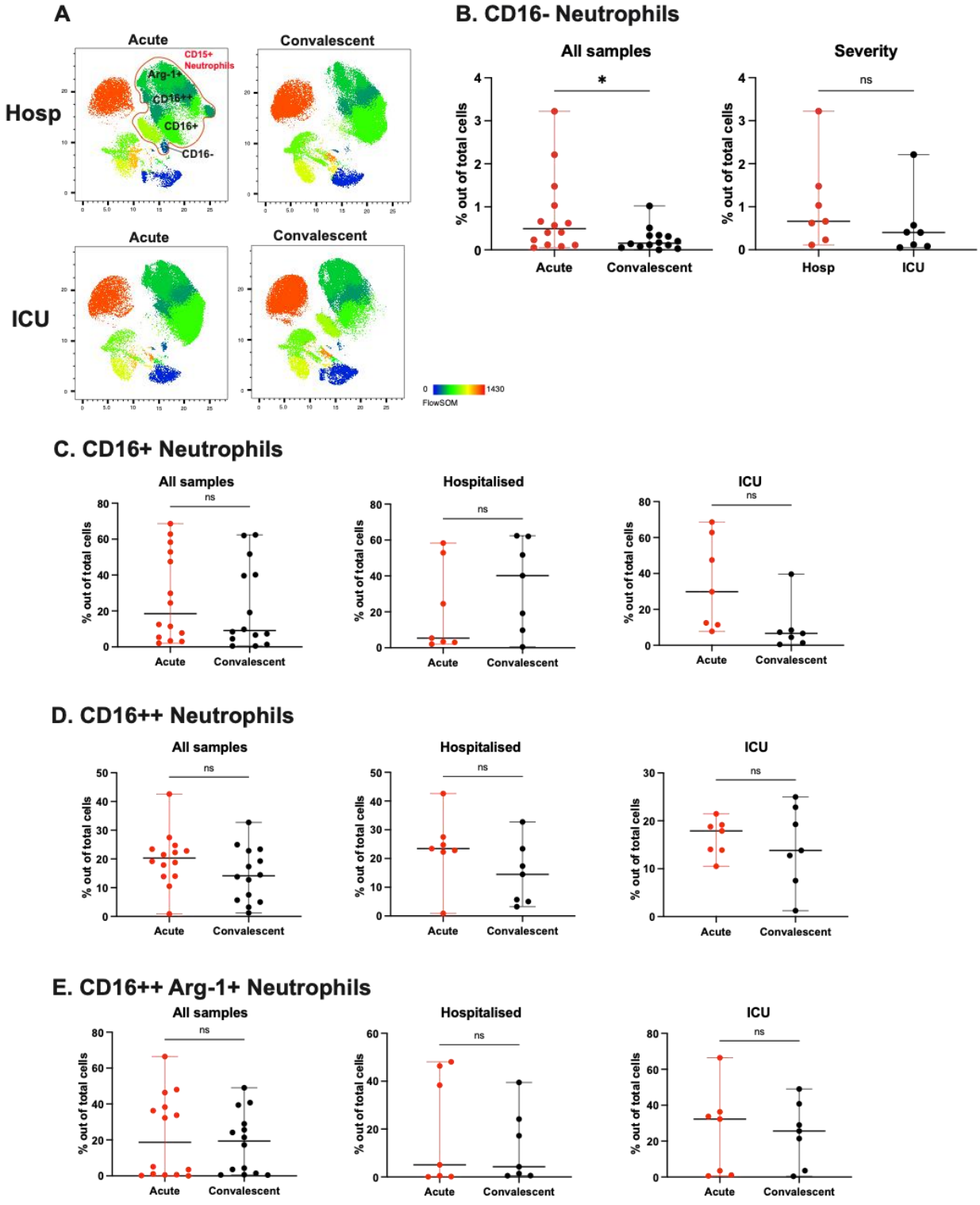

Figure 15: Variation in the detection of neutrophil sub-population. (A) UMAP projection of different subgroups among hospitalised and ICU COVID-19 samples with FlowSOM metaclusters overlaid. (B)-(E) Percentage of neutrophil subpopulations of total cells according to FlowSOM metaclusters, $CD16^{-}$ (B); $CD16^{+}$ (C); $CD16^{++}$ (D); $CD16^{++}$ $ARG1^{+}$ (E). Statistical analysis was done with the Wilcoxon matched-pair signed rank test for nonparametric data. *,p ≤0.05; **,p ≤0.01; ***,p ≤0.001.

5. Discussion

This study used flow cytometry to investigate the performance of four commercial whole blood cryopreserving stabilisers on maintaining leukocyte surface markers. Our main finding was that the detectability of well-defined and highly expressed immune cell lineages was reasonably accurate in preserved samples. Nevertheless, depending on targeted markers, fluorescence intensity varied between different stabilisers as well as between stabilisers and fresh controls. There was no single best stabiliser that worked for all cell types. Different cell types, markers, antibody clones, processing time and techniques decided the best suitable stabilisers.

5.1. Immunophenotyping of cryopreserved whole blood.

Whole blood freezing offers an alternative to the standard procedure – PBMC isolation and cryopreservation with cryo-protectants. Though widely used, the multi-step and time-consuming process of PBMC preparation could alter cellular characteristics[91]. Additionally, it eliminates high-density cells such as granulocytes, which represents 70% of total leukocytes. Whereas, whole blood cryopreservation offers 1) a rapid process that minimizes changes in cellular structures after the removal of physiological environments; 2) a simple and inexpensive procedure that requires a smaller sample volume than PBMCs and allows a collection of many samples simultaneously without highly trained staff and complex equipment; 3) cell fixation making the method safe for highly infectious samples such as COVID-19 or Ebola; 4) a good representation of whole blood composition by retaining granulocyte populations.

To date, our study is the first comprehensive analysis of multiple whole blood cryopreserving reagents for flow cytometry. Using cryopreserved samples is a common practice, but most studies used PBMC fraction only and focused on immune subsets' viability and functional capacity, particularly lymphocytes post cryopreservation. Since the whole blood cryopreservation is efficient and straightforward, multiple efforts have been made to test its validity in multicenter or field immunophenotyping studies. However, these studies mainly focused on major immune lineages or specific markers with one to two whole blood stabilising reagents. Some notable studies include 1) comparison between Phosphoflow Fix

and Lyse, and PROT-1 for profiling lineage markers in flow cytometry and mass cytometry by Rybakowska P. *et al.*[83]; 2) cryopreservation method to study granulocyte activation developed by Ruiter K.D *et al.*[25]; (3) mass cytometry analysis of whole blood stabilisers on chemokine receptors by Sakkestad ST *et al*.[92]. This study sought to expand on their work, investigating the performance of stabilising reagents - Cytodelics, PROT-1, SLSS-V2, and Transfix for flow cytometry analysis of neutrophils and their activation markers, monocytes, B cells, NK cells and T cell subpopulations. The workflow adhered to manufacturers' recommendation, and all the staining were done using antibody cocktails to minimize staining variability between samples.

5.2. Antibody staining after fixation

Staining post-fixation and cryopreservation might cause high background staining. As samples were fixed and cryo-preserved right after the collection, it was impossible to exclude dead cells before the staining. Dead cells could take up antibodies non-specifically and have a high autofluorescence, subsequently interfering with data interpretation. Nevertheless, the amount of cell death was probably small since the interval between the blood drawing and sample processing was reasonably short. Moreover, the fixation process for all stabilisers had a minimal procedure of one to two times pipetting and a short incubation at RT.

Staining post-fixation was challenging due to a loss of signal or false positives. Fixation and permeabilization could alter antigen structures or generate unspecific binding sites[93]. All stabilisers here use formaldehyde as a primary fixative, which makes non-selective crosslinks between proteins. These crosslinks might lead to changes in three-dimensional conformations of target proteins, thus reducing their immunoreactivity with antibodies. While over-fixation could cause excessive cross-linking, under-fixation could result in unequal crosslinks between the cell surface and intracellular locations, making them more susceptible to cryo-damages.[94]

Moreover, all the studied antibodies here were monoclonal, each of which bound to only one epitope on target antigens. If the cross-linking by fixatives impaired that structure, it would generate false-negative events. This explained why the markers in this study, such as CD16 and CD11b (Figure 6 and Figure 11) were sensitive to antibody clones since each clone

recognises only one epitope. From our experience, PROT-1 seemed to preserve antigen structures more robustly than Cytodelics since the latter only worked for a much smaller selection of antibody clones, or otherwise it would result in a reduction or even a complete loss of MFI signal. Thus, fixation time, antibody clones and titration need to be considered carefully during panel optimisation.

5.3. Antigenic detection after fixation and cryopreservation

5.3.1. Effects of fix/freeze/stain workflow

The workflow of all studied whole blood stabilisers followed a fix/freeze/stain procedure. The process could introduce several technical biases, such as fixing/freezing/thawing time and temperature. The detection of antigens was also dependent on individual marker sensitivity to fixation and cryopreservation as mentioned above. Our results showed that highly expressed markers endured the fixing and freezing process better than low-expressed antigens, which was in agreement with previous studies[83,95]. This might be owing to both their abundance and more stable nature.

In addition, fixing and freezing altered cell morphologies as indicated in FSC and SSC profiles compared to fresh control. The most affected cells were monocytes and granulocytes, which are in agreement with previous studies[25,83,96]. Despite that, Cytodelics, PROT-1 and Transfix offered clear segregation of granulocytes, monocytes and lymphocytes comparable to the fresh control.

5.3.2. Robust preservation of major lymphocyte subsets

Our result demonstrated that cryopreserving reagents – Cytodelics, PROT-1, and Transfix reduced fluorescence intensity but maintained similar percentages of major lymphocyte subsets to those obtained with the standard stain/fix/lyse procedure of BD Facs Lysing solution (Figure 8). T, B and NK cells were correctly detected across all the stabilisers. These results are in line with a previous study done by Pinto *et al.* that the freezing of fixed whole blood made no dramatic alteration to the frequency of lymphocyte subsets despite a reduction in signal intensity[95]. There was a slight decrease in CD16 signal, but the detection

of NK cell subsets based on CD16 was comparable to the controls. The trend was in contrast with the previous finding that a reduced CD16 signal hindered the determination of monocyte subsets[83]. This might be due to different antibody clones and sample processing methods.

5.3.3. Hampered separation of T cell sub-population

Here we reported how the four whole blood cryopreservation kits performed for γδ T cells and sub-population of CD4 and CD8 T cells. For γδ T cells, better results were obtained in Transfix, and the data more closely resembled PBMC than the fresh control. On the other hand, Cytodelics, PROT-1 and SLSS-V2 caused a significant reduction in TCR-γδ signal, making it impossible to distinguish between negative and positive events. The fixatives in these reagents might have destroyed binding sites for the antibody. One solution is to replace our current B1 clone with gamma3.20 or H-41 for TCR γδ. These clones were extensively studied and confirmed to work with Formalin-Fixed Paraffin-Embedded Tissues, indicating that it might work with formaldehyde fixation found in all the stabilisers[97]. Unfortunately, we have found no directly fluorochrome-conjugated antibody for flow cytometry having either of these clones. However, it might be possible to stain cells with a primary antibody bearing these clones, followed by a fluorochrome-conjugated secondary antibody.

The determination of α/β CD4 and CD8 T cell subsets was challenging owing to the lower CCR7 signal. Here we were unable to identify correctly naïve, recent thymic emigrants, central memory, effector memory and terminally differentiated effector memory cells using these four stabilisers. Formaldehyde fixation and cryopreservation had detrimental effects on CCR7 signal resolution as shown in Figure 10. The attenuation of CCR7 signal was reported before, but mainly on mass cytometry data[92,98].

The CCR7 signal separation was entirely lost on CD4 population, making it impossible to distinguish between naïve and memory subsets. However, the situation was improved with CD8 where Cytodelics and PROT-1 maintained the frequency of T cell subsets comparable to the controls. It was not clear why CCR7 on CD4 and CD8 behaved differently. One possible explanation was due to the abundance of CCR7 on each subset. Despite that, the distribution of CD4 subsets deviated far from acceptable ranges. Thus, CCR7 or most likely also other

chemokine receptors, in general, are not suitable for fix/freeze/stain procedure, specifically for these whole blood stabilisers[92].

5.3.4. Unreliable detection of monocyte composition

When testing deeper immunophenotyping of innate cell populations, we could not distinguish monocyte subsets reliably in all cryopreserved samples due to the partial loss of CD14 signal intensity. Cytodelics showed to be the most suitable stabilisers for classical monocytes, followed by PROT-1 and Transfix. One approach to improve the signal intensity could be to use a brighter fluorochrome than PerCP-Cy5.5. Although our current clone was validated by Cytodelics' manufacturer, switching antibody clones and increasing antibody titration might also help.

SLSS-V2 was problematic for monocytes. Not only having a reduced signal intensity, SLSS-V2 also caused a significant shift in cell morphologies, as indicated by the shift in FSC/SSC profiles. Changing PMT voltages of FSC and SSC yielded no improvement for the separation of monocytes and granulocytes. The issue might be due to harsh fixation and lysis in SLSS-V2 during the freezing process. It might also be a trade-off for a more straightforward thawing process – SLSS-V2 protocol only required two washing steps while preserving samples at more versatile temperatures than other stabilisers.

5.3.5. Perpetuation of neutrophil activation status

Our study showed that Cytodelics, PROT-1 and, Transfix maintained the activation status of neutrophils after fMLP and LPS stimulation. The elevation of CD66b, CD11b and CD16 and reduction of CD62L were clearly observed in samples treated with these stabilisers, with one exception of CD11b in Cytodelics, which required another antibody clone for reliable detection. However, the proportion of change in CD11b, CD16, and CD62L was comparable to the controls only in PROT-1 preserved samples stimulated with LPS. Cytodelics allowed a correct quantification of changes in CD16 and to a lesser extend in CD11b when a correct antibody clone was used (data not shown). In addition, CD66b signal was weak in all stabilisers compared to the controls, indicating that CD66b was not suitable for studying in fixed and frozen samples, which is in agreement with the previous report[25]. In addition to that, all tested

activation markers were poorly detected in SLSS-V2 and to some extent in Transfix. Therefore, PROT-1 and Cytodelics would be more suitable for preserving neutrophils' activation status.

PROT-1 and Cytodelics conserved neutrophil activation status regardless of differences in MFI and proportion of MFI changes compared with the unfixed control. The finding is in line with a previous study done by Ruiteet *et al.*, where they examined neutrophil activation markers following fix/freeze/stain procedure[25]. Our study contributed further to the field with an understanding of how effective four commercial cryopreservation kits are for granulocytes and how much the proportion of MFI changes in the aforementioned activation markers deviated in fixed and cryopreserved samples. This discrepancy indicates that PROT-1 and Cytodelics did not fully capture the scale of activation and cellular changes in neutrophils.

While the controls showed a similar cellular change between fMLP and LPS stimulation, the fixed and cryopreserved samples demonstrated that LPS activated neutrophils more than fLMP (Figure 12). The difference could be due to a massive amount of cell death after fMLP treatment (data not shown). The 1-hour treatment of fLMP might have been harsh on cells, reduced viability and possibly altered antigenic structures. In our preliminary study, 5-minute stimulation with fMLP was sufficient to activate neutrophils. 1-hour time point was used to simplify the experimental workflow.

5.4. Whole blood cryopreservation for flow cytometry and mass cytometry

Mass Cytometry or Cytometry by Time-Of-Flight (CyTOF) and flow cytometry (FC) are widely used for immunophenotyping. They both detect numerous parameters at a single-cell level. However, whole blood cryopreservation by Cytodelics, PROT-1, and SLSS-V2 are more widely used in CyTOF than in FC. The limitations of fluorochrome technology make antigenic detection in fixed and frozen samples more challenging. First, FC is less sensitive and prone to error due to spillover and autofluorescence. Correction for spectral overlap requires compensation, which could introduce variation to data interpretation. High-dimension FC panels increase the complexity of compensation matrix, making it more prone to the loss of signal resolution. Second, FC can also take cell-associated autofluorescence into analysis. Thus, fluorescence spillover and autofluorescence background are detrimental to detecting

low abundance antigens, particularly when their sensitivity to antibody staining has been reduced by fixation and cryopreservation.[99,100]

On the other hand, CyTOF has higher sensitivity while requiring little or no compensation. CyTOF has a low background since it uses a time-of-flight mass spectrometer to analyse element isotopes that label antibodies instead of fluorochromes. A minimal background with no spectral spillover and correction in CyTOF allows excellent discrimination of negative and positive populations even with low signal intensity.[101]

These differences in underlying technologies of FC and CyTOF might explain the discrepancy in the detection of certain antigens. For example, we were unable to reliably identify CD62L and CD14 signals in Cytodelics-fixed samples, contrary to our previous study where detection was done using CyTOF[102]. However, the loss of signal was often observed in the FC detection of markers expressed at low levels, whereas highly expressed markers were impacted less. Thus, Cytodelics or PROT-1 can be used for FC with consideration of cellular or antigenic targets and thorough testing.

5.5. Application in COVID-19

5.5.1. Reliable detection of major immune subsets from cryopreserved prospective samples from COVID-19 patients

Analysis of 14 patients with longitudinal samples preserved in Cytodelics revealed the striking differences in T cells, monocytes, and neutrophils between acute and convalescent phases. Hospitalised and ICU patients had an abnormally low number of CD3 T cells during the acute infection, indicating lymphopenia often found in severe cases[103]. In addition, the reduction of $CD14^+$ monocyte, mainly classical monocytes, during the early SARS-COV-2 infection in severe patients was similar to a previous finding[104]. Cytodelics also allowed detection of emergency granulopoiesis during the acute phase, as indicated by an increase in both total $CD15^+$ neutrophils and their immature compartment. These findings are in agreement with the current understanding of immune responses in COVID-19[104–106]. Identifying these differences further confirms that Cytodelics preserved highly expressed lineage markers sufficiently for immunophenotyping by flow cytometry.

5.5.2. Inadequate detection of temporal changes in neutrophil sub-population

FlowSOM clustering identified different subsets of neutrophils in Cytodelics-preserved patient samples. The unsupervised analysis confirmed the heterogeneity of neutrophil populations during the SARS-COV-2 infection. Our result showed that early progression of COVID-19 was marked with the expansion of $CD16^{-}$ immature neutrophils, which was also reported previously by Reusch *et al.*[75]. However, our flow cytometry panel could not identify some apoptotic and non-functional neutrophils which might be included in $CD16^{-}$ immature neutrophils[107].

On the other hand, no significant difference was observed for other neutrophil subsets between the acute and convalescent phases of either hospitalised or ICU patients. Particularly, a similar trend was found for suppressive neutrophils which was identified as Lin^{-} $CD15^{+}$ $CD11b^{+}$ $CD33^{low/+}$ HLA-$DR^{-/low}$ LOX-1^{+} $ARG1^{+}$ PD-$L1^{+}$ in FlowSOM cluster 3 (Figure 15E). Moreover, no dramatic difference was detected even if FlowSOM clustering was iterated with a higher number of clusters (data not shown). The finding did not resemble current literature on the expansion of this suppressive neutrophil population during the early phase of SARS-COV-2 infection[108,109]. Our relatively small patient cohort might have been insufficient to detect a statistical significance, although some studied subjects displayed strikingly high levels of these suppressive cells. On the other hand, 21 to 90 days might not have been enough for suppressive neutrophils to return to their normal level since Sieminska et al. reported that mild and asymptomatic COVID-19 had MDSCs persisting in convalescence, even three months after the infection[110]. However, further study is needed to understand why some studied subjects had these suppressive neutrophils increased significantly (Figure 15E).

Identifying suppressive neutrophils in whole blood samples is challenging due to biological heterogeneity of neutrophils and technical limitations. Both immature MDSC and mature populations can display suppressive functions[37]. There is currently no consensus on how to identify suppressive neutrophils or MDSC from whole blood. While Apodaca *et al.* suggested that whole blood yields the most accurate results[111], others have argued that G-MDSC should only be analysed from PBMC fractions[33,112]. Moreover, our results show LOX-1 is expressed at different levels across neutrophil subsets instead of only in suppressive population as has been suggested before[89]. In addition, ARG1 has been reported to be released by normal neutrophils upon activation[38]. In other words, LOX-1 and ARG1 might not

be sufficient to differentiate suppressive neutrophils from other neutrophil populations, particularly in COVID-19 patients.

On the other hand, unsupervised analysis using our current flow cytometry panel might be insufficient to detect suppressive populations. Signal intensity of all markers was not equal, making it more difficult to detect very dim signals with FlowSOM clustering and UMAP visualisation[113]. For example, extremely low signal PD-L1 appeared negative on the heatmap for FlowSOM metaclusters. More preprocessing steps could be used, e.g. FlowAI/FlowClean for cleaning data or Cytonorm for data normalisation in addition to downsampling and the removal of debris, singlets, and eosinophils[114–116]. This could help to reduce further background signal and normalise signal intensity for unsupervised analysis. However, there would be a risk of over-transformation of the data since the compensation had transformed it already beforehand. On the other hand, automated analysis might fail to identify a population that accounts for less than 5% of the total cells[117]. Suppressive neutrophil frequencies vary between individuals. Particularly in some patients, the numbers can be tiny, making them challenging to detect. In conclusion, it is not straightforward to identify this population in cryo-preserved whole blood samples. A further study with a bigger cohort and better data processing is needed to the issue.

5.6. Conclusion and future perspectives

All in all, the aforementioned commercial whole blood stabilising kits can be used for immunophenotyping in flow cytometry. There are various approaches to continue this project and improve the efficacy of these stabilisers.

First, further optimisations are needed to increase the efficacy of these whole blood stabilisers for low abundance markers. One approach is to stain samples before adding stabilising buffers. A stain/fix/freeze procedure would reduce the detrimental effects of formaldehyde fixation on epitope structures, thus preserving their immunoreactivity with antibodies. Moreover, antibody staining before cryopreservation can incorporate dead cell markers to access sample viability and decrease unspecific staining. However, the stain/fix/freeze workflow might risk complicating the sample collection, particularly in clinics where nurses or staffs have limited time and facility to do antibody staining.

Next, it would be interesting to investigate how these whole blood stabilisers preserve intracellular markers for immune phenotyping in flow cytometry. After being thawed and stained for surface markers, samples can be permeabilized by detergents e.g. saponin, and then stained for intracellular markers. However, it is unclear if the stabilising buffers can cause cell permeabilization and how it could affect the staining of intracellular markers. Therefore, selection of compatible antibodies and experimental workflow is essential to achieve the best result.

Lastly, we plan to analyse a bigger cohort of COVID-19 patients to determine if Cytodelics is suitable for studying granulocytes. The current patient cohort is small, with only 14 patients, and immune profiles are highly variable between individuals. As a result, it is inconclusive if our negative findings on different granulocyte subsets in COVID-19 were entirely due to Cytodelics and our workflow or it is because of patient-to-patient variation. Moreover, we plan to look deeper into the clinical data of some patients displaying a high level of suppressive neutrophils, as shown in Figure 15E. It might be possible to determine if there is any underlying clinical data differentiating them from other patients.

In conclusion, this thesis provided an in-depth analysis on the detectability of a wide range of cell surface makers fixed and cryopreserved in Cytodelics, PROT-1, SLSS-V2 and Transfix. Although fixation and cryopreservation altered fluorescence intensity, antibody affinity and cell morphology, PROT-1, Cytodelics and Transfix allow robust identification of major immune lineages by flow cytometry. Notably, rapid sample processing with minimal requirements of facility makes them a valuable tool for field studies, especially for infectious diseases like COVID-19.

6. Acknowledgement

First of all, I would like to thank my supervisors, Eliisa and Santtu for giving me the opportunities to do this project. Thank you, Eliisa, for teaching me so much about research and immunology and answering all my questions, even the tiniest ones. Thank you for letting me participate in other projects besides my master thesis and learn many new things. Thank you, Santtu, for being so supportive and patient, trying to help whenever I need. And I really appreciate that you are so generous financially :D and give me a lot of space and independence to learn and grow as a scientist.

I am grateful for the financial support from the University of Helsinki for my master study, and Samsung Dream Foundation and Yonsei University, which have laid a strong foundation for me to pursue higher education.

I would like to express my gratitude to all the donors and patients who have provided precious samples, making this study possible.

Thank you, Nelli, Iivari, Kirsten, Xiaobo, Shamita and Joona for being my wonderful lab mates, teaching me lab techniques and being so open to my questions. I love all the moments shared with you guys, from a little talk over the lab bench to our lunches and Fika. You all are adorable and inspiring scientists ☺☺ I would like to thank Tomas, and Luz for showing me new ideas and teaching me about granulocytes. Warm thanks to Marjo and Tamas for being there and helping me with experiments. In addition, I want to acknowledge all my colleagues at the Translational Immunology Research program, Virology department, COVID-19 sample collection team.

My sincere appreciation to Tiina, our Transmed captain, for your advice and supports. Thank you for being so welcoming and understanding, teaching me how to deal with difficult situations.

Most importantly, I would like to thank my family and monkey sisters for showing me love and perseverance. Thank you for cherishing me and being a shoulder I could lean on whenever things get tough. And thanks for being so smart and kind-hearted, teaching me to love learning and live boldly.

Thank you, my dear Henrik. No words can describe how lucky and happy I am to be with you. Thanks for moving to Finland for my master and being patient with all my ups and downs during this thesis. I would also like to thank Patrik, Bjorn and Nella for supporting our decisions.

Thank you, my 'into the wood' friends, Minea, Veera, Neja and Feli, for sharing every step of this thesis and master program with me. Thank you, Phuong, for bringing me so much joy and taste of Vietnam here in Finland. You guys have made Finland such a lovely place for me. Thank you, Quynh and Khanh, for being my besties and standing by me regardless of time and distance. You both have made my time doing thesis during the pandemic so much more breathable and happier.

I would like to thank all my Transmed classmates, my friends in Vietnam and Korea, and many more people I could not name all here, who have helped me financially and emotionally throughout this master program.

References

1. Box, A. *et al.* Evaluating the Effects of Cell Sorting on Gene Expression. *J. Biomol. Tech.* **31**, 100–111 (2020).
2. Maecker, H. T., McCoy, J. P. & Nussenblatt, R. Standardizing immunophenotyping for the Human Immunology Project. *Nat. Rev. Immunol.* **12**, 191–200 (2012).
3. de Jong, E. & Bosco, A. Unlocking immune-mediated disease mechanisms with transcriptomics. *Biochem. Soc. Trans.* **49**, 705–714 (2021).
4. Behbehani, G. K. Immunophenotyping by Mass Cytometry. *Methods Mol. Biol.* **2032**, 31–51 (2019).
5. Campana, D. & Behm, F. G. Immunophenotyping of leukemia. *J. Immunol. Methods* **243**, 59–75 (2000).
6. Janols, H. *et al.* Lymphocyte and monocyte flow cytometry immunophenotyping as a diagnostic tool in uncharacteristic inflammatory disorders. *BMC Infect. Dis.* **10**, 205 (2010).
7. Bonilla, D. L., Reinin, G. & Chua, E. Full Spectrum Flow Cytometry as a Powerful Technology for Cancer Immunotherapy Research. *Front Mol Biosci* **7**, 612801 (2020).
8. Neo, S. Y., O'Reilly, A. & Pico de Coaña, Y. Immune Monitoring of Cancer Patients by Multi-color Flow Cytometry. *Methods Mol. Biol.* **1913**, 49–65 (2019).
9. Akira, S. Innate immunity and adjuvants. *Philos. Trans. R. Soc. Lond. B Biol. Sci.* **366**, 2748–2755 (2011).
10. Medzhitov, R. & Janeway, C., Jr. Innate immunity. *N. Engl. J. Med.* **343**, 338–344 (2000).
11. Sarma, J. V. & Ward, P. A. The complement system. *Cell Tissue Res.* **343**, 227–235 (2011).
12. Kenneth M Murphy, C. W. *The adaptive immune response - Janeway's Immunobiology - 9th Edition*. 345–493 (Garland Science, Taylor & Francis Group, LLC, 2017).
13. Murphy, K. & Weaver, C. Integrated dynamics of innate and adaptive immunity. *Janeway's Immunobiology, 9th Edition. New York and London: Garland Science* 445–488 (2017).
14. King, K. Y. & Goodell, M. A. Inflammatory modulation of HSCs: viewing the HSC as a foundation for the immune response. *Nat. Rev. Immunol.* **11**, 685–692 (2011).

15. Ziegler-Heitbrock, L. Blood Monocytes and Their Subsets: Established Features and Open Questions. *Front. Immunol.* **6**, 423 (2015).

16. Kapellos, T. S. *et al.* Human Monocyte Subsets and Phenotypes in Major Chronic Inflammatory Diseases. *Front. Immunol.* **10**, 2035 (2019).

17. Ziegler-Heitbrock, L. Monocyte Subsets: Phenotypes and Function in Tuberculosis infection. *Frontiers in imunology* **6**, 423 (2015).

18. Shi, C. & Pamer, E. G. Monocyte recruitment during infection and inflammation. *Nat. Rev. Immunol.* **11**, 762–774 (2011).

19. Twomey, J. J., Douglass, C. C. & Sharkey, O., Jr. The monocytopenia of aplastic anemia. *Blood* **41**, 187–195 (1973).

20. Lower, E. E. & Baughman, R. P. The effect of cancer and chemotherapy on monocyte function. *J. Clin. Lab. Immunol.* **31**, 121–125 (1990).

21. Ley, K. *et al.* Neutrophils: New insights and open questions. *Sci Immunol* **3**, (2018).

22. Summers, C. *et al.* Neutrophil kinetics in health and disease. *Trends Immunol.* **31**, 318–324 (2010).

23. Kolaczkowska, E. & Kubes, P. Neutrophil recruitment and function in health and inflammation. *Nat. Rev. Immunol.* **13**, 159–175 (2013).

24. Cecilia Johansson, F. C. M. K. Neutrophils in respiratory viral infections. *Mucosal Immunology* **14**, 815–827 (2021).

25. de Ruiter, K. *et al.* A field-applicable method for flow cytometric analysis of granulocyte activation: Cryopreservation of fixed granulocytes. *Cytometry A* **93**, 540–547 (2018).

26. Kenneth M Murphy, C. W. *Janeway's Immunobiology - 9th Edition*. 345–493 (Garland Science, Taylor & Francis Group, LLC, 2017).

27. Papayannopoulos, V. Neutrophil extracellular traps in immunity and disease. *Nat. Rev. Immunol.* **18**, 134–147 (2018).

28. Malech, H. L., Deleo, F. R. & Quinn, M. T. The role of neutrophils in the immune system: an overview. *Methods Mol. Biol.* **1124**, 3–10 (2014).

29. Minns, D., Smith, K. J., Hardisty, G., Rossi, A. G. & Gwyer Findlay, E. The Outcome of Neutrophil-T Cell Contact Differs Depending on Activation Status of Both Cell Types. *Front. Immunol.* **12**, 633486 (2021).

30. Vono, M. *et al.* Neutrophils acquire the capacity for antigen presentation to memory CD4+ T cells in vitro and ex vivo. *Blood* **129**, 1991–2001 (2017).

31. Puga, I. *et al.* B cell-helper neutrophils stimulate the diversification and production of immunoglobulin in the marginal zone of the spleen. *Nat. Immunol.* **13**, 170–180 (2011).

32. Gabrilovich, D. I. *et al.* The terminology issue for myeloid-derived suppressor cells. *Cancer research* vol. 67 425; author reply 426 (2007).

33. Bronte, V. *et al.* Recommendations for myeloid-derived suppressor cell nomenclature and characterization standards. *Nat. Commun.* **7**, 12150 (2016).

34. Gabrilovich, D. I. Myeloid-Derived Suppressor Cells. *Cancer Immunol Res* **5**, 3–8 (2017).

35. Aarts, C. E. M. *et al.* Activated neutrophils exert myeloid-derived suppressor cell activity damaging T cells beyond repair. *Blood Adv* **3**, 3562–3574 (2019).

36. Sagiv, J. Y. *et al.* Phenotypic diversity and plasticity in circulating neutrophil subpopulations in cancer. *Cell Rep.* **10**, 562–573 (2015).

37. Pillay, J., Tak, T., Kamp, V. M. & Koenderman, L. Immune suppression by neutrophils and granulocytic myeloid-derived suppressor cells: similarities and differences. *Cell. Mol. Life Sci.* **70**, 3813–3827 (2013).

38. Rodriguez, P. C. *et al.* Arginase I-producing myeloid-derived suppressor cells in renal cell carcinoma are a subpopulation of activated granulocytes. *Cancer Res.* **69**, 1553–1560 (2009).

39. Millrud, C. R., Bergenfelz, C. & Leandersson, K. On the origin of myeloid-derived suppressor cells. *Oncotarget* **8**, 3649–3665 (2017).

40. Munder, M. *et al.* Arginase I is constitutively expressed in human granulocytes and participates in fungicidal activity. *Blood* **105**, 2549–2556 (2005).

41. Rodriguez, P. C., Quiceno, D. G. & Ochoa, A. C. L-arginine availability regulates T-lymphocyte cell-cycle progression. *Blood* **109**, 1568–1573 (2007).

42. Feldmeyer, N. *et al.* Arginine deficiency leads to impaired cofilin dephosphorylation in activated human T lymphocytes. *Int. Immunol.* **24**, 303–313 (2012).

43. Werner, A. *et al.* Reconstitution of T Cell Proliferation under Arginine Limitation: Activated Human T Cells Take Up Citrulline via L-Type Amino Acid Transporter 1 and Use It to Regenerate Arginine after Induction of Argininosuccinate Synthase Expression. *Front. Immunol.* **8**, 864 (2017).

44. Kim, S.-H., Roszik, J., Grimm, E. A. & Ekmekcioglu, S. Impact of l-Arginine Metabolism on Immune Response and Anticancer Immunotherapy. *Front. Oncol.* **8**, 67 (2018).

45. Chen, X., Song, M., Zhang, B. & Zhang, Y. Reactive Oxygen Species Regulate T Cell Immune Response in the Tumor Microenvironment. *Oxid. Med. Cell. Longev.* **2016**, 1580967 (2016).

46. Cooper, M. A., Fehniger, T. A. & Caligiuri, M. A. The biology of human natural killer-cell subsets. *Trends Immunol.* **22**, 633–640 (2001).

47. Stabile, H., Fionda, C., Gismondi, A. & Santoni, A. Role of Distinct Natural Killer Cell Subsets in Anticancer Response. *Front. Immunol.* **8**, 293 (2017).

48. Amand, M. *et al.* Human CD56dimCD16dim Cells As an Individualized Natural Killer Cell Subset. *Front. Immunol.* **8**, 699 (2017).

49. Guillerey, C., Huntington, N. D. & Smyth, M. J. Targeting natural killer cells in cancer immunotherapy. *Nat. Immunol.* **17**, 1025–1036 (2016).

50. Chaplin, D. D. Overview of the immune response. *J. Allergy Clin. Immunol.* **125**, S3-23 (2010).

51. Janeway, C. A., Jr, Travers, P., Walport, M. & Shlomchik, M. J. *The Humoral Immune Response*. (Garland Science, 2001).

52. Golubovskaya, V. & Wu, L. Different Subsets of T Cells, Memory, Effector Functions, and CAR-T Immunotherapy. *Cancers* **8**, (2016).

53. Luckheeram, R. V., Zhou, R., Verma, A. D. & Xia, B. CD4+T Cells: Differentiation and Functions. *Clin. Dev. Immunol.* **2012**, (2012).

54. Zhang, N. & Bevan, M. J. CD8(+) T cells: foot soldiers of the immune system. *Immunity* **35**, 161–168 (2011).

55. Andersen, M. H., Schrama, D., Thor Straten, P. & Becker, J. C. Cytotoxic T cells. *J. Invest. Dermatol.* **126**, 32–41 (2006).

56. Wong, P. & Pamer, E. G. CD8 T cell responses to infectious pathogens. *Annu. Rev. Immunol.* **21**, 29–70 (2003).

57. Fink, P. J. The biology of recent thymic emigrants. *Annu. Rev. Immunol.* **31**, 31–50 (2013).

58. Hassan, J. & Reen, D. J. Human recent thymic emigrants–identification, expansion, and survival characteristics. *The Journal of Immunology* (2001).

59. Ravkov, E., Slev, P. & Heikal, N. Thymic output: Assessment of CD4+ recent thymic emigrants and T-Cell receptor excision circles in infants. *Cytometry B Clin. Cytom.* **92**, 249–257 (2017).

60. Sckisel, G. D. *et al.* Out-of-Sequence Signal 3 Paralyzes Primary CD4(+) T-Cell-Dependent Immunity. *Immunity* **43**, 240–250 (2015).

61. Martin, M. D. & Badovinac, V. P. Defining Memory CD8 T Cell. *Front. Immunol.* **9**, 2692 (2018).

62. Gustafsson, K., Herrmann, T. & Dieli, F. Editorial: Understanding Gamma Delta T Cell Multifunctionality - Towards Immunotherapeutic Applications. *Front. Immunol.* **11**, 921 (2020).

63. Lawand, M., Déchanet-Merville, J. & Dieu-Nosjean, M.-C. Key Features of Gamma-Delta T-Cell Subsets in Human Diseases and Their Immunotherapeutic Implications. *Front. Immunol.* **8**, 761 (2017).

64. Ribot, J. C., Lopes, N. & Silva-Santos, B. γδ T cells in tissue physiology and surveillance. *Nat. Rev. Immunol.* **21**, 221–232 (2021).

65. Yuki, K., Fujiogi, M. & Koutsogiannaki, S. COVID-19 pathophysiology: A review. *Clin. Immunol.* **215**, 108427 (2020).

66. Tay, M. Z., Poh, C. M., Rénia, L., MacAry, P. A. & Ng, L. F. P. The trinity of COVID-19: immunity, inflammation and intervention. *Nat. Rev. Immunol.* **20**, 363–374 (2020).

67. Jin, Y. *et al.* Virology, Epidemiology, Pathogenesis, and Control of COVID-19. *Viruses* **12**, (2020).

68. Lee, I. T. *et al.* ACE2 localizes to the respiratory cilia and is not increased by ACE inhibitors or ARBs. *Nat. Commun.* **11**, 5453 (2020).

69. Scudellari, M. How the coronavirus infects cells - and why Delta is so dangerous. *Nature* **595**, 640–644 (2021).

70. Yap, J. K. Y., Moriyama, M. & Iwasaki, A. Inflammasomes and Pyroptosis as Therapeutic Targets for COVID-19. *J. Immunol.* **205**, 307–312 (2020).

71. Kim, Y.-M. & Shin, E.-C. Type I and III interferon responses in SARS-CoV-2 infection. *Exp. Mol. Med.* **53**, 750–760 (2021).

72. Peñaloza, H. F., Lee, J. S. & Ray, P. Neutrophils and lymphopenia, an unknown axis in severe COVID-19 disease. *PLoS Pathog.* **17**, e1009850 (2021).

73. Cavalcante-Silva, L. H. A. *et al.* Neutrophils and COVID-19: The road so far. *Int. Immunopharmacol.* **90**, 107233 (2021).

74. Ackermann, M. *et al.* Patients with COVID-19: in the dark-NETs of neutrophils. *Cell Death Differ.* (2021) doi:10.1038/s41418-021-00805-z.

75. Reusch, N. *et al.* Neutrophils in COVID-19. *Front. Immunol.* **12**, 652470 (2021).

76. Verschoor, C. P., Kohli, V. & Balion, C. A comprehensive assessment of immunophenotyping performed in cryopreserved peripheral whole blood. *Cytometry B Clin. Cytom.* **94**, 662–670 (2018).

77. Lotfi, M., Hamblin, M. R. & Rezaei, N. COVID-19: Transmission, prevention, and potential therapeutic opportunities. *Clin. Chim. Acta* **508**, 254–266 (2020).

78. Meryman, H. T. Cryopreservation of living cells: principles and practice. *Transfusion* **47**, 935–945 (2007).

79. Oh, H., Siano, B. & Diamond, S. Neutrophil isolation protocol. *J. Vis. Exp.* (2008) doi:10.3791/745.

80. Ekpenyong, A. E., Toepfner, N., Chilvers, E. R. & Guck, J. Mechanotransduction in neutrophil activation and deactivation. *Biochim. Biophys. Acta* **1853**, 3105–3116 (2015).

81. Vian, A. M. & Higgins, A. Z. Membrane permeability of the human granulocyte to water, dimethyl sulfoxide, glycerol, propylene glycol and ethylene glycol. *Cryobiology* **68**, 35–42 (2014).

82. Takahashi, T., Hammett, M. F. & Cho, M. S. Multifaceted freezing injury in human polymorphonuclear cells at high subfreezing temperatures. *Cryobiology* **22**, 215–236 (1985).

83. Rybakowska, P. *et al.* Stabilization of Human Whole Blood Samples for Multicenter and Retrospective Immunophenotyping Studies. *Cytometry A* **99**, 524–537 (2021).

84. Bashratyan, R. *et al.* Tools to simplify panel design for multi-color flow cytometry experiments. *The Journal of Immunology* **198**, 81.22-81.22 (2017).

85. Group Samples by Antibody. FlowJo for antibody titrations: Separation index and concatenation. https://www.uwhealth.org/files/uwhealth/docs/cancer_for_researchers/Flow/FlowJo-Antibody-Titrations.pdf.

86. Van Gassen, S. *et al.* FlowSOM: Using self-organizing maps for visualization and interpretation of cytometry data. *Cytometry A* **87**, 636–645 (2015).

87. Kalina, T. *et al.* EuroFlow standardization of flow cytometer instrument settings and immunophenotyping protocols. *Leukemia* **26**, 1986–2010 (2012).

88. Johnston, L. Whole Blood Cryopreservation and The Discovery of an Alternative Blocking Method. https://voices.uchicago.edu/ucflow/2019/11/11/whole-blood-cryopreservation-and-the-discovery-of-an-alternative-blocking-method/.

89. Condamine, T. *et al.* Lectin-type oxidized LDL receptor-1 distinguishes population of human polymorphonuclear myeloid-derived suppressor cells in cancer patients. *Sci Immunol* **1**, (2016).

90. Zea, A. H. *et al.* Arginase-producing myeloid suppressor cells in renal cell carcinoma patients: a mechanism of tumor evasion. *Cancer Res.* **65**, 3044–3048 (2005).

91. Brodin, P. & Davis, M. M. Human immune system variation. *Nat. Rev. Immunol.* **17**, 21–29 (2017).

92. Sakkestad, S. T., Skavland, J. & Hanevik, K. Whole blood preservation methods alter chemokine receptor detection in mass cytometry experiments. *J. Immunol. Methods* **476**, 112673 (2020).

93. Pilch-Cooper, H. A. *et al.* Circulating human CD4 and CD8 T cells do not have large intracellular pools of CCR5. *Blood* **118**, 1015–1019 (2011).

94. Ramos-Vara, J. A. & Miller, M. A. When tissue antigens and antibodies get along: revisiting the technical aspects of immunohistochemistry--the red, brown, and blue technique. *Vet. Pathol.* **51**, 42–87 (2014).

95. Pinto, L. A. *et al.* Fixation and cryopreservation of whole blood and isolated mononuclear cells: Influence of different procedures on lymphocyte subset analysis by flow cytometry. *Cytometry B Clin. Cytom.* **63**, 47–55 (2005).

96. Nemes, E. *et al.* Differential leukocyte counting and immunophenotyping in cryopreserved ex vivo whole blood. *Cytometry A* **87**, 157–165 (2015).

97. Jungbluth, A. A. *et al.* Immunohistochemical Detection of γ/δ T Lymphocytes in Formalin-fixed Paraffin-embedded Tissues. *Appl. Immunohistochem. Mol. Morphol.* **27**, 581–583 (2019).

98. Nassar, A. F., Wisnewski, A. V. & Raddassi, K. Automation of sample preparation for mass cytometry barcoding in support of clinical research: protocol optimization. *Anal. Bioanal. Chem.* **409**, 2363–2372 (2017).

99. Roederer, M. Spectral compensation for flow cytometry: visualization artifacts, limitations, and caveats. *Cytometry* **45**, 194–205 (2001).

100. Baumgarth, N. & Roederer, M. A practical approach to multicolor flow cytometry for immunophenotyping. *J. Immunol. Methods* **243**, 77–97 (2000).

101. Cheung, R. K. & Utz, P. J. Screening: CyTOF-the next generation of cell detection. *Nat. Rev. Rheumatol.* **7**, 502–503 (2011).

102. Rodriguez, L. *et al.* Systems-Level Immunomonitoring from Acute to Recovery Phase of Severe COVID-19. *Cell Rep Med* **1**, 100078 (2020).

103. Tavakolpour, S., Rakhshandehroo, T., Wei, E. X. & Rashidian, M. Lymphopenia during the COVID-19 infection: What it shows and what can be learned. *Immunol. Lett.* **225**, 31–32 (2020).

104. Mathew, D. *et al.* Deep immune profiling of COVID-19 patients reveals distinct immunotypes with therapeutic implications. *Science* **369**, (2020).

105. Lagunas-Rangel, F. A. Neutrophil-to-lymphocyte ratio and lymphocyte-to-C-reactive protein ratio in patients with severe coronavirus disease 2019 (COVID-19): A meta-analysis. *J. Med. Virol.* **92**, 1733–1734 (2020).

106. Meizlish, M. L. *et al.* A neutrophil activation signature predicts critical illness and mortality in COVID-19. *Blood Adv* **5**, 1164–1177 (2021).

107. Dransfield, I. *et al.* Neutrophil apoptosis is associated with a reduction in CD16 (Fc gamma RIII) expression. *J. Immunol.* **153**, 1254–1263 (1994).

108. Sacchi, A. *et al.* Early expansion of myeloid-derived suppressor cells inhibits SARS-CoV-2 specific T-cell response and may predict fatal COVID-19 outcome. *Cell Death Dis.* **11**, 921 (2020).

109. Veglia, F., Sanseviero, E. & Gabrilovich, D. I. Myeloid-derived suppressor cells in the era of increasing myeloid cell diversity. *Nat. Rev. Immunol.* (2021) doi:10.1038/s41577-020-00490-y.

110. Siemińska, I. *et al.* Mild and Asymptomatic COVID-19 Convalescents Present Long-Term Endotype of Immunosuppression Associated With Neutrophil Subsets Possessing Regulatory Functions. *Front. Immunol.* **12**, 3931 (2021).

111. Apodaca, M. C. *et al.* Characterization of a whole blood assay for quantifying myeloid-derived suppressor cells. *Journal for ImmunoTherapy of Cancer* **7**, 230 (2019).

112. Kotsakis, A. *et al.* Myeloid-derived suppressor cell measurements in fresh and cryopreserved blood samples. *J. Immunol. Methods* **381**, 14–22 (2012).

113. Folcarelli, R. *et al.* Transformation of multicolour flow cytometry data with OTflow prevents misleading multivariate analysis results and incorrect immunological conclusions. *Cytometry A* (2021) doi:10.1002/cyto.a.24491.

114. Monaco, G. *et al.* flowAI: automatic and interactive anomaly discerning tools for flow cytometry data. *Bioinformatics* **32**, 2473–2480 (2016).

115. Van Gassen, S., Gaudilliere, B., Angst, M. S., Saeys, Y. & Aghaeepour, N. CytoNorm: A Normalization Algorithm for Cytometry Data. *Cytometry A* **97**, 268–278 (2020).

116. Fletez-Brant, K., Špidlen, J., Brinkman, R. R., Roederer, M. & Chattopadhyay, P. K. flowClean: Automated identification and removal of fluorescence anomalies in flow cytometry data. *Cytometry Part A* vol. 89 461–471 (2016).

117. Pedreira, C. E. *et al.* Overview of clinical flow cytometry data analysis: recent advances and future challenges. *Trends Biotechnol.* **31**, 415–425 (2013).